

TEXTBOOK SERIES

VOLUME 2

WELL TESTING

by

Zoltán E. HEINEMANN
Professor for Reservoir Engineering
Leoben, October 2005

actualized

by

Dr. Georg Mittermeir
Tehran, February 2013

For kind Attention

The Textbook series of the PHDG is an aid for PhD students accepted by the Association or those applying for support from it. These scripts have the objective to stabilize and homogenize the knowledge of the candidates, not necessarily studied petroleum engineering and originating from different countries and universities.

The textbooks are subject to continuous update and improvement. PHDG suggests to download them in yearly sequence. In some cases they are provided on different levels of knowledge making it easier to enter the subjects. Therefore there is also some overlapping between the volumes. It is expected that the users will suggest improvements for both, the contents and the formulations.

PHDG's Textbooks available at 1.1.2015:

1. Fluid Flow in Porous Medium
2. Well Testing
3. Systematic of the Reservoir Flow Equations
4. Introduction to Reservoir Simulation
5. Natural Fractured Reservoir Engineering

PHDG Textbooks in preparation, intended to be issued during 2015:

1. Discretization and Gridding in Reservoir Simulation
2. Advanced Reservoir Simulation
3. Reservoir Fluid Characterisation

Supplementary scripts used at the Montanuniversität up to the retirement of Professor Zoltán E. Heinemann in July 2006.

1. Reservoir Fluids
2. Petroleum Recovery

© No part of this publication may be reproduced in any form.

Not applicable as teaching material at universities or any other kind of courses without prior, written permission of the PHDG association. Students of the following universities can ask for free copies for personal use: Sharif University of Technology, Tehran University, Iran University of Science and Technology, Shiraz University, University of Miskolc, Montanuniversität Leoben.

Table of Contents

1 Introduction	1
1.1. Methods	1
1.2. Evaluation of Formation Tests	6
1.3. Productivity Index	11
1.4. Skin Effect	11
1.5. Principle of Superposition	15
1.6. Wellbore Storage	17
1.7. Pressure Change	21
1.7.1 Drainage Radius	27
1.7.2 Multi-Phase Filtration	27
1.7.3 Equations for Gas-Flow	28
2 Pressure Drawdown Analysis.....	33
2.1. Semilog Plot	33
2.2. Type Curve Matching	34
2.3. Reservoir Limit Testing	35
3 Pressure Build Up Curve	43
3.1. Horner Plot	43
3.2. Type Curve Matching	45
3.3. Skin Factor	46
3.4. Reservoir Pressure	47
3.5. Gas Producing Wells	51
4 Multiple Well Testing.....	55
4.1. Interference Test	55
4.2. Pulse Test	58
5 Nomenclature.....	69
6 References.....	71
7 Appendix.....	73

List of Figures

Figure 1.1:	Pressure drop in a production well inside a finite reservoir	2
Figure 1.2:	Pressure distribution inside a quadratic reservoir with two wells. (From Matthews and Russel ^[11])	3
Figure 1.3:	Production test at an increasing production rate	3
Figure 1.4:	Production test at an decreasing production rate	4
Figure 1.5:	Pressure buildup measurement	4
Figure 1.6:	Pressure response for an interference test	5
Figure 1.7:	Pressure response for a pulse test	5
Figure 1.8:	Dimensionless pressure for a single well in an infinite radial system. Solution according to Equation 1.30 (no skin, no wellbore storage).	10
Figure 1.9:	Skin zone of finite thickness (after EARLOUGHER ^[4])	12
Figure 1.10:	Infinitely acting reservoir with several wells	15
Figure 1.11:	Effect of wellbore storage on sand face flow rate	19
Figure 1.12:	Type-curves for a single well inside a homogenous reservoir with wellbore storage and skin effects (after BOURDET et al. ^[2])	23
Figure 1.13:	Log-log plot vs. (after BOURDET et al. ^[2])	24
Figure 1.14:	Type curves - homogenous reservoir with wellbore storage and skin (after BOURDET et al. ^[2])	26
Figure 1.15:	Dimensionless pressure for a well in the center of a closed circular reservoir, no wellbore storage, no skin (EARLOUGHER and RAMEY ^[5])	30
Figure 1.16:	Dimensionless pressure for a single well in various closed rectangular systems, no wellbore storage, no skin (EARLOUGHER and RAMEY ^[5])	30
Figure 1.17:	Dimensionless pressure for a single well in various closed rectangular systems, no wellbore storage, no skin (EARLOUGHER and RAMEY ^[5])	31
Figure 2.1:	Evaluation of the transient pressure drop (after MATTHEWS and RUSSEL ^[11])	33
Figure 2.2:	Semilog plot of pressure drawdown data	39
Figure 2.3:	Reservoir limit testing for pressure drawdown data	40
Figure 3.1:	Pressure buildup curve with skin effect and wellbore storage	44
Figure 3.2:	Pressure buildup curve with a limited drainage area	48
Figure 3.3:	MBH dimensionless pressure for a well in the center of equilateral drainage areas (after MATTHEWS-BRONS-HAZENBROEK ^[10])	52
Figure 3.4:	MBH dimensionless pressure for different well locations in a square drainage area (after MATTHEWS-BRONS-HAZENBROEK ^[10])	53
Figure 4.1:	Illustration of type curve matching for an interference test (after EARLOUGHER ^[4]) ..	56
Figure 4.2:	Schematic illustration of rate (pulse) history and pressure response for a pulse test ..	59
Figure 4.3:	Schematic pulse-test rate and pressure history showing definition of time and pulse response amplitude.	60
Figure 4.4:	Pulse testing: relation between time lag and response amplitude for first odd pulse (after KAMAL and BRIGHAM ^[7])	61
Figure 4.5:	Pulse testing: relation between time lag and response amplitude for first even pulse (after KAMAL and BRIGHAM ^[7])	62
Figure 4.6:	Pulse testing: relation between time lag and response amplitude for all odd pulses except the first pulse (after KAMAL and BRIGHAM ^[7])	63

Figure 4.7: Pulse testing: relation between time lag and response amplitude for all even pulses except the first pulse (after KAMAL and BRIGHAM ^[7])	64
Figure 4.8: Pulse testing: relation between time lag and cycle length for the first odd pulse (after KAMAL and BRIGHAM ^[7])	65
Figure 4.9: Pulse testing: relation between time lag and cycle length for the first even pulse (after KAMAL and BRIGHAM ^[7])	66
Figure 4.10: Pulse testing: relation between time lag and cycle length for all odd pulses except the first pulse (after KAMAL and BRIGHAM ^[7])	66
Figure 4.11: Pulse testing: relation between time lag and cycle length for all even pulses except the first pulse (after KAMAL and BRIGHAM ^[7])	67

1 Introduction

In a well, which opens a hydrocarbon or water-bearing layers, the bottom-hole pressure can be measured during production and during a following shut in period. From these data, conclusions can be drawn about the reservoir, the efficiency of the *sand face perforation* and about the quantitative relationship between production rate and bottom-hole pressure.

Wells interfere with each other. Opening or shut-in a well causes pressure changes in neighboring wells. They can be recorded with high precision, whereby the permeability and porosity of a reservoir can be determined.

Hydrodynamic well tests, also called formation tests, have a basic significance. They allow to determine the state of reservoirs and wells and help to optimize production and recovery. Formation tests can be carried out in an uncased bore-hole (this is a drillstem test) as well as in a completed well. The methods differ, but the basic principles remain the same.

In wildcat, exploration, and appraisal wells, economical, environmental and safety considerations often constrain the applicable methods and the duration of the tests severely. This can limit the knowledge we can gain from the well. However, tests performed before the onset of field production have distinguished advantage because the reservoir may remain in a single phase state throughout the test duration. When the first wells are drilled in a virgin reservoir representative fluid samples can be collected. In most of the cases, only these samples are representative for PVT (dependency of pressure-volume-temperature) analysis. Once the field has been produced and the oil reservoir pressure has dropped below the bubble point or the gas reservoir pressure below the dew point, it is not possible anymore to determine the original fluid composition.

The two basic categories of well tests are *transient* and *stabilized* tests. The goal of the stabilized tests is to determine a relationship between the average pressure of the drainage area, the bottom hole pressure and the production rate, in other words, to determine the productivity index.

In this textbook, the most important methods of well tests and their evaluations are presented. For the theoretical basis, reference is made to the textbook "*Fluid Flow in Porous Media*"^[6]. For more in depth study, the SPE Monographs from Matthews and Russel^[11], Earlougher^[4] and Lee^[8] are recommended.

1.1. Methods

During the production of a well at a constant rate, the bottom-hole pressure decreases continuously (Figure 1.1).

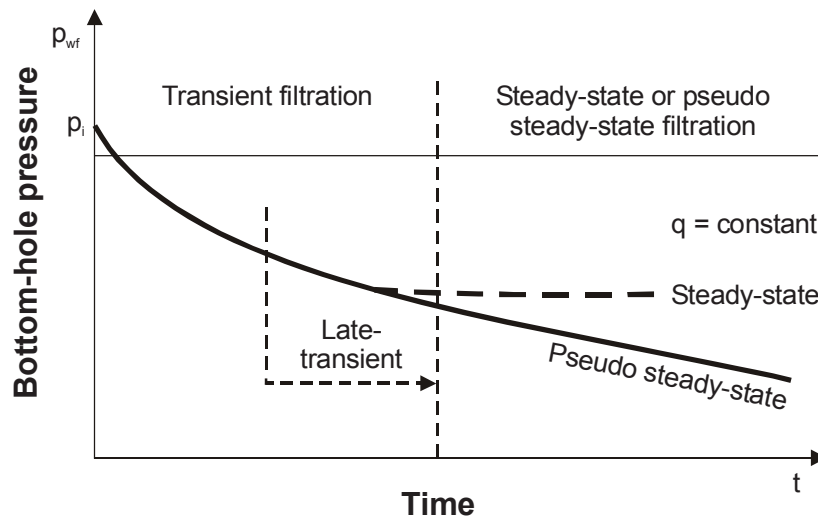


Figure 1.1: Pressure drop in a production well inside a finite reservoir

At the beginning, the pressure decrease is especially quick, but with time becomes more and more moderate. Beyond a certain point, the pressure curve can become linear. This point divides the curve into two parts:

- transient and
- steady state or pseudo-steady state period.

The filtration is steady state if no more pressure changes occur. This indicates that the formation has a boundary with constant pressure. The pressure distribution between this boundary and the well casing is constant. A linear change of the bottom-hole pressure indicates a finite drainage area. The production is the consequence of the fluid expansion within this area.

The drainage area of a well is determined by its share in the total production the formation. If there is only one well, the drainage area is identical with the reservoir. In transient conditions, the drainage area changes. Figure 1.2 shows the pressure distribution in a theoretically homogenous square shaped reservoir with two production wells. The bottom hole pressures are not shown for either well, these are far below the bottom of the sketch. The ratio of production rates is 1:2.

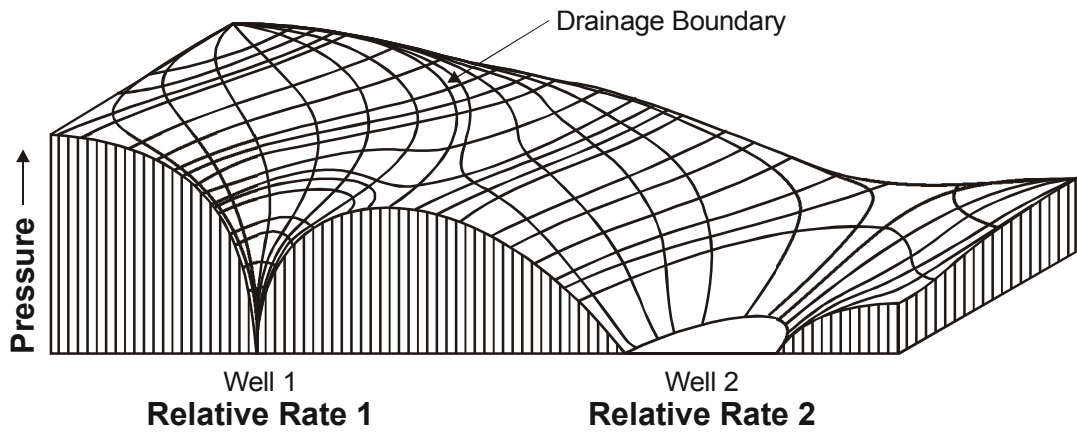


Figure 1.2: Pressure distribution inside a quadratic reservoir with two wells (From Matthews and Russel^[11])

If the production rate is changing during the tests, the pressure change is also more complicated. Fig 1.3 shows a test with a rate increasing in steps, whereas Figure 1.4 shows a test with a rate decreasing in steps. If the time periods are short, the pressure change remains transient.

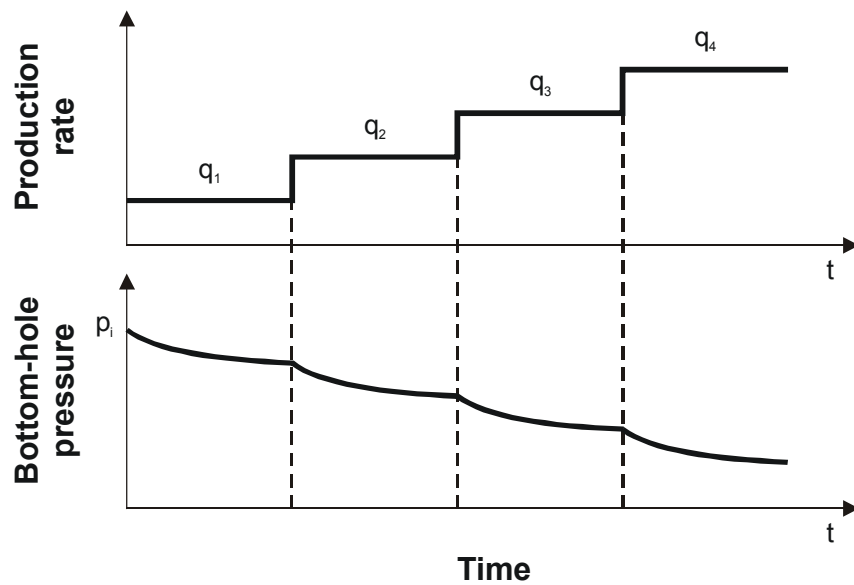


Figure 1.3: Production test at an increasing production rate

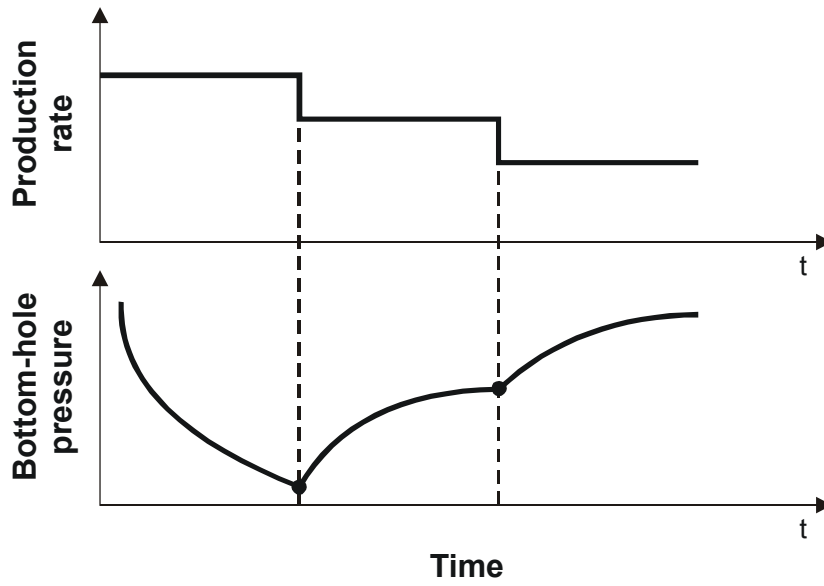


Figure 1.4: Production test at an decreasing production rate

Among the possible tests, the pressure buildup test has a special significance. After producing at constant rate, production is stopped and the pressure buildup is measured (Figure 1.5).

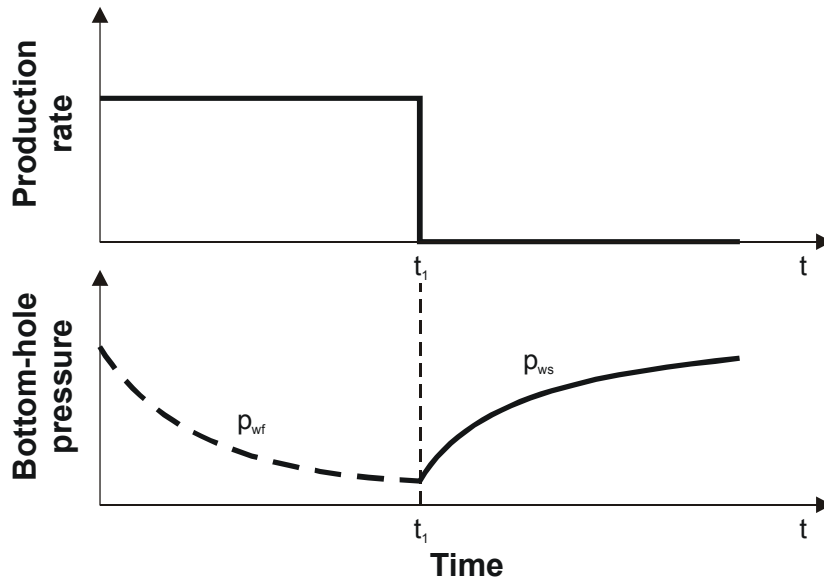


Figure 1.5: Pressure buildup measurement

Figure 1.6 shows an interference test. While the active well produces at a constant rate, the observation well is shut in. The pressure in the observation well increases at first (in the case of an earlier production) and then decreases due to the influence of the active well.

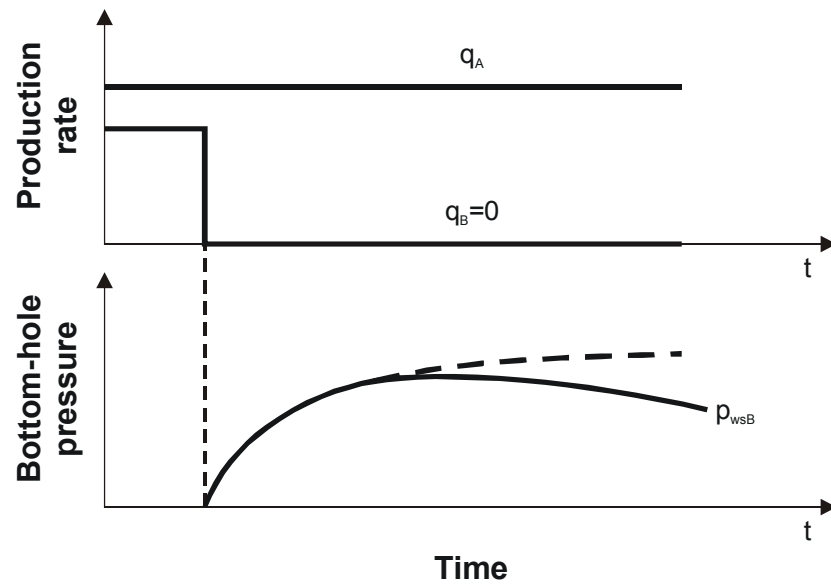


Figure 1.6: Pressure response for an interference test

It is possible to produce periodically from the active well, as shown in Figure , i.e. the well *pulsates*. The pressure changes in the observation well are very small, but can still be recorded by a differential manometer. The time lag between the *pulse* and the *answer* is in relation to the product of porosity and total compressibility of the formation.

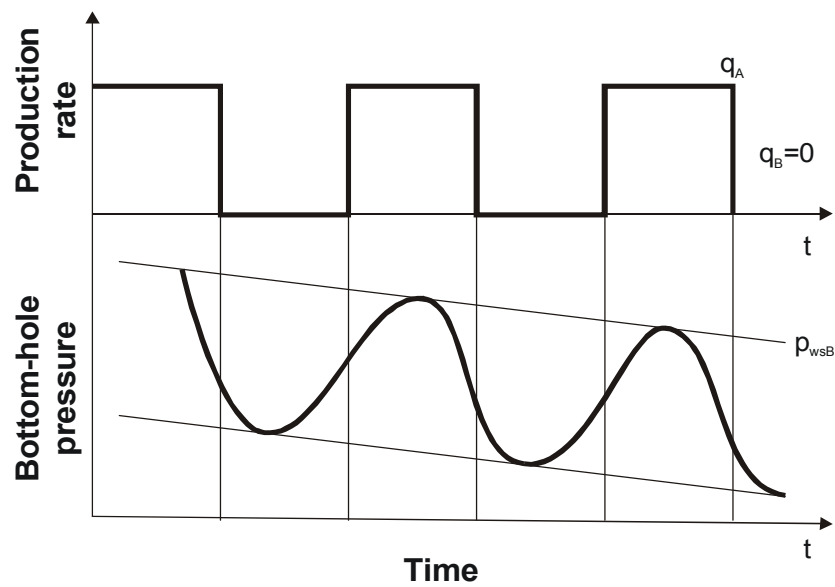


Figure 1.7: Pressure response for a pulse test

1.2. Evaluation of Formation Tests

In Section 1.1 filtration states were characterized as transient, steady state and pseudo-steady state. These terms are derived from theoretical hydrodynamics and designate the dependence of these processes on time. For the purpose of evaluating a formation test, we need a mathematical model which sets up a quantitative relationship between the production rate, the pressure and the parameters of the reservoir and of the fluid.

The success of a formation test can be assured by the coordination of three elements:

- the object,
- the measurement,
- the mathematical model.

None of these three elements is definitive. Measurements can be carried out at different states of objective reservoirs and wells. A test should be conducted only if the states fulfill the conditions of the mathematical model used for the evaluation. The tests should be accomplished in such a way that the pressure change at the given location and during the evaluated time period is determined by only one (or at least by only a few) unknown parameters of the system.

The evaluation always takes place on the basis of a solution of the mathematical model. The application of *dimensionless variables* often makes the evaluation easier. These are

the dimensionless radius

$$r_D = r/r_w, \quad (1.1)$$

the dimensionless time

$$t_D = \frac{kt}{\phi\mu c_t r_w^2}, \quad (1.2)$$

or

$$t_{DA} = t_D \left(\frac{r_w^2}{A} \right) \quad (1.3)$$

and the dimensionless pressure

$$p_D(t_D, r_D) = \frac{2\pi hk}{qB\mu} [p(t, r) - p_i], \quad (1.4)$$

where

- k - the permeability
 ϕ - the porosity
 μ - the fluid viscosity
 c_t - the effective compressibility
 r_w - the radius of the well
 A - the drainage area surface
 h - the formation thickness
 q - the flow rate
 B - the formation volume factor
 p_i - the initial pressure

In field units Equation 1.2-Equation 1.4 are written in the following form:

$$t_D = \frac{0.0002637kt}{\phi\mu c_t r_w^2} \quad (1.5)$$

$$t_{DA} = \frac{0.60536 \times 10^{-8} kt}{\phi\mu c_t A} \quad (1.6)$$

$$p_D(t_D, r_D) = \frac{0.00708hk}{qB\mu} [p(t, r) - p_i]. \quad (1.7)$$

p_D is, in contrast to its designation, a pressure difference. The pressure $p(r, t)$ value is calculated from the model, therefore p_D always refers to the solution and not to the measured pressure difference.

In the case of formation tests, the pressure measured at the place of production (or of injection), the bottom-hole pressure, has a special significance. Here $r = r_w$, thereby $r_D = 1$, and these conditions are specially designated for the dimensionless pressure:

$$p_{Dw}(t_D) = p_D(t_D, r_D = 1) + s \quad (1.8)$$

The quantity s is a dimensionless pressure change defined as the *skin* factor.

As a matter of fact, the permeability in the immediate vicinity of the well deviates from the original one, due to the influence of the filtrate and the formation opening. Usually it is smaller and causes an additional pressure drop. If $p_{wf}(t)$ is the bottom hole flowing pressure, Equation 1.4 and Equation 1.7 lead to the following definition:

$$p_{Dw}(t_D) = \frac{2\pi hk}{q\mu B} [p_{wf}(t) - p_i] \quad (1.9)$$

This is the reason why $p_{Dw}(t_D)$ is not equal to $p_D(t_D, r_D = 1)$. For field units, 2π has to be replaced with the constant 0.00708.

Example 1.1

In an infinite acting reservoir, a well produces $40 \text{ m}^3/d$ [$251.5 \text{ bbl}/d$] oil for five days. p_{wf} is to be calculated without considering a skin effect ($s = 0$). The dimensionless pressure for the homogeneous, infinite acting reservoir, with constant well rate is given in Figure 1.8.

The data are

$$\begin{aligned}
 p_i &= 33.24 \text{ MPa} [4819.8 \text{ psi}] \\
 B_o &= 1.52 [] \\
 \mu_o &= 1.28 \times 10^{-3} \text{ Pa s} [1.28 \text{ cP}] \\
 h &= 12 \text{ m} [39.37 \text{ ft}] \\
 q &= -40 \text{ m}^3/d = -0.463 \times 10^{-3} \text{ m}^3/s [-251.5 \text{ bbl}/d] \\
 t &= 5 \text{ d} = 0.432 \times 10^{-6} \text{ s} \\
 k_o &= 0.16 \times 10^{-12} \text{ m}^2 [160 \text{ mD}] \\
 \phi &= 0.18 [] \\
 c_t &= 3.86 \times 10^{-9} \text{ Pa}^{-1} [2.662 \times 10^{-5} \text{ 1/psi}] \\
 r_w &= 0.1 \text{ m} [0.328 \text{ ft}]
 \end{aligned}$$

Solution:

From Equation 1.2:

$$\begin{aligned}
 t_D &= \frac{kt}{\phi \mu c_t r_w^2} \\
 t_D &= \frac{0.16 \times 10^{-12} \times 432000 \text{ m}^2 \text{ s Pa}}{0.18 \times 1.28 \times 10^{-3} \times 3.86 \times 10^{-9} \times 0.1^2 \text{ Pa s m}^2} \\
 t_D &= 7.77 \times 10^6 [-]
 \end{aligned}$$

The dimensionless well radius is $r_D = 1$ and $(t_D/r_D^2) = 7.77 \times 10^6$. From Figure 1.8, the dimensionless pressure can be read, $p_D = 8.0$. We use Equation 1.9 for computing the bottom hole pressure:

$$\begin{aligned}(p_{wf})_{ideal} &= \frac{q\mu B}{2\pi hk} p_D + p_i \\ &= \frac{-0.463 \times 10^{-3} \times 1.52 \times 1.28 \times 10^{-3}}{2\pi \times 12 \times 0.16 \times 10^{-12}} \times 8 + 33.24 \times 10^6\end{aligned}$$

$$(p_{wf})_{ideal} = 32.64 \text{ MPa}$$

In field units:

$$(p_{wf})_{ideal} = \frac{-251.5 \times 1.28 \times 1.52}{0.00708 \times 39.37 \times 160} \times 8 + 4819.8 = 4732 \text{ psi}$$

The index *ideal* implies that no skin effect was considered.

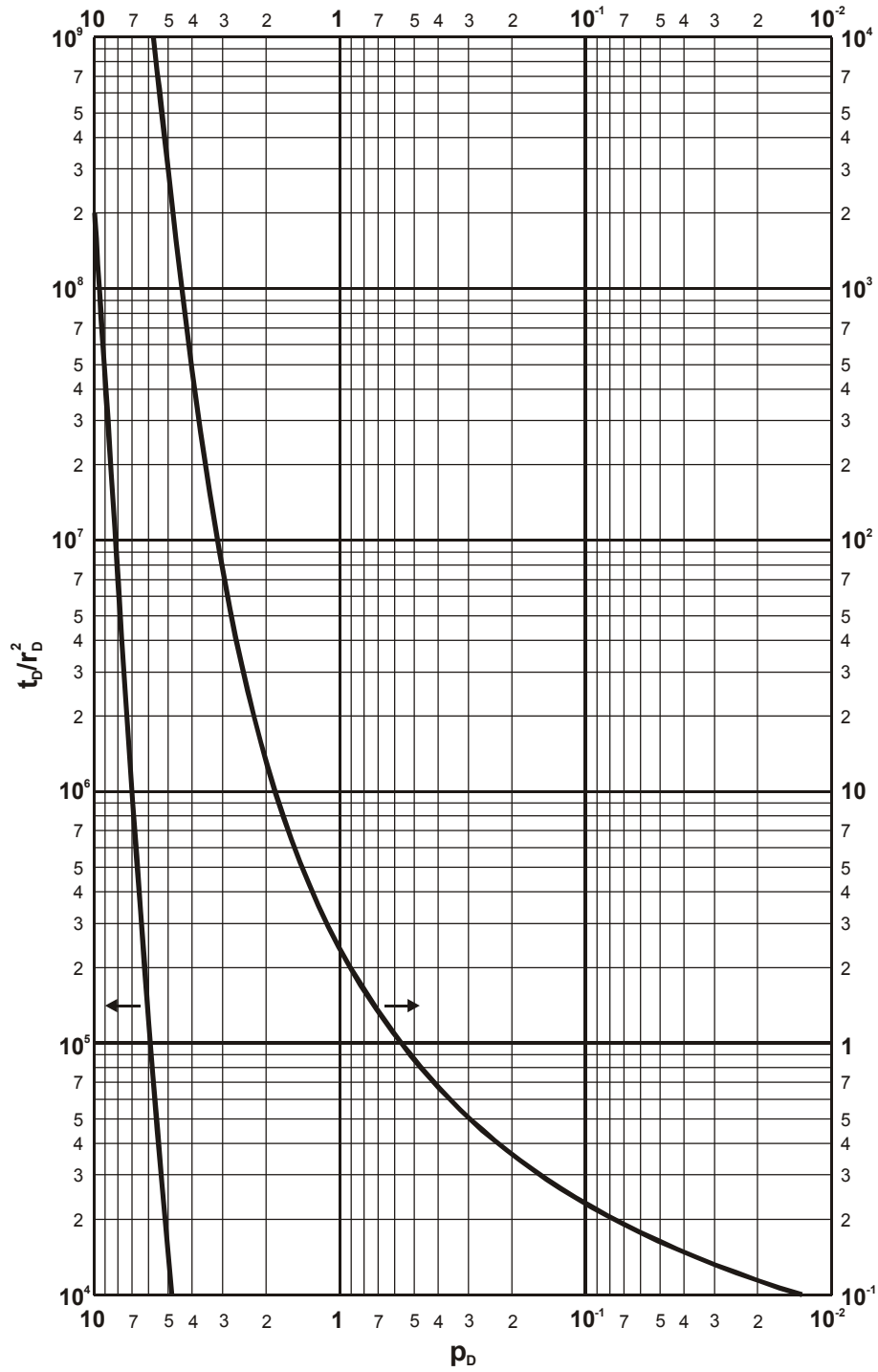


Figure 1.8: Dimensionless pressure for a single well in an infinite radial system. Solution according to Equation 1.30 (no skin, no wellbore storage).

1.3. Productivity Index

A well produces or injects with rate q . As consequence, there is a potential difference between the well bottom and an arbitrary point in the formation. For a horizontal formation this can be expressed as a difference of pressures at the same depth:

$$\Delta p(t) = p_{wf}(t) - p(r, t). \quad (1.10)$$

It is obvious that the production rate is a function of this pressure difference:

$$q = f(\Delta p) \quad (1.11)$$

and $q \rightarrow 0$ if $\Delta p \rightarrow 0$.

The productivity index is defined as

$$J = \lim_{\Delta p \rightarrow 0} \left(\frac{q}{\Delta p} \right). \quad (1.12)$$

For practical purposes, the productivity index can be approximated with finite values:

$$J = \frac{q}{\Delta p}. \quad (1.13)$$

1.4. Skin Effect

The rock properties around a well normally deviate from the original ones, due to the influence of the mud filtrate, the well completion and the formation opening (see Figure 1.9). This altered zone is called "skin zone" and has a radius r_s and a permeability k_s . For this radius pseudo steady-state flow can be assumed and therefore the *Dupuit* equation can be applied:

$$q = \frac{2\pi h k_s \Delta p_s}{\mu B \ln \frac{r_s}{r_w}}, \quad (1.14)$$

or if $k_s = k$, i.e. no skin effects,

$$q = \frac{2\pi h k \Delta p}{\mu B \ln \frac{r_s}{r_w}}, \quad (1.15)$$

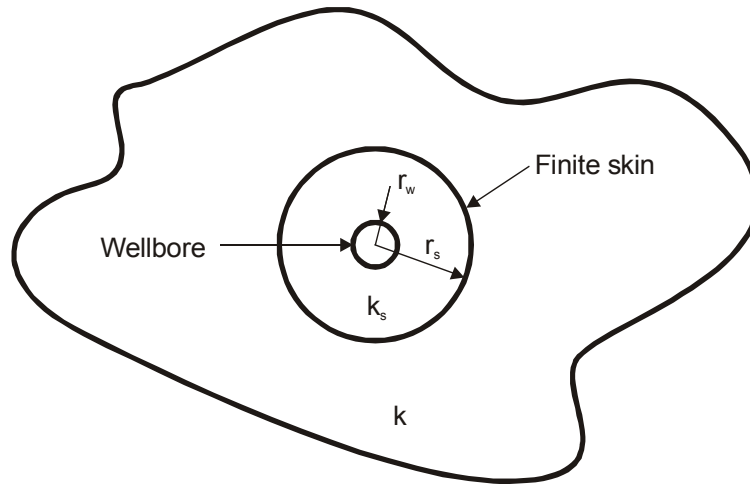


Figure 1.9: Skin zone of finite thickness (after EARLOUGHER^[4])

where

- Δp is the pressure drop over the radius $r_w \leq r \leq r_s$ with the original permeability and
- Δp_s - the same with changed permeability.

Let be

$$\Delta p_{skin} = (p_{wf})_{real} - (p_{wf})_{ideal} \quad (1.16)$$

the supplementary pressure drop over the "skin zone". It is evident that this can be expressed by the pressure differences too:

$$\Delta p_{skin} = \Delta p_s - \Delta p \quad (1.17)$$

Then following from Equation 1.4 and Equation 1.9:

$$\Delta p_{skin} = \frac{q\mu B}{2\pi h k} s. \quad (1.18)$$

Inserting Δp_s , Δp and Δp_{skin} from Equation 1.14, Equation 1.15 and Equation 1.18 into Equation 1.16 it follows:

$$s = \left(\frac{k}{k_s} - 1 \right) \ln \frac{r_s}{r_w}. \quad (1.19)$$

Equation 1.19 is called *Hawkins* formula. Based on this equation the dimensionless skin factor s could be calculated if both r_s and k_s were known. This is never the case, therefore traditionally the supplementary pressure drop Δp_{skin} will be regarded as it would occur just on the well

surface. This means that the altered zone is imagined as a skin on this surface. The skin factor s is positive if $k_s \leq k$. If a formation treatment is carried out with success, it is possible that $k_s > k$, and then s is negative.

The values r_s and k_s cannot be determined from the value s simultaneously. This difficulty can be eliminated by introducing an *apparent well radius* r_{wa} . The radius r_{wa} would cause the same pressure drop without skin as the real well radius r_w with a skin. For that, the following condition must be fulfilled:

$$\ln \frac{r_e}{r_{wa}} = \ln \frac{r_e}{r_w} + s, \quad (1.20)$$

thus

$$r_{wa} = r_w e^{-s}. \quad (1.21)$$

The values s and r_{wa} are not descriptive enough, therefore a *flow efficiency* and a *damage factor* are defined. Flow efficiency:

$$FE = \frac{J_{actual}}{J_{ideal}} = \frac{\bar{p} - p_{wf} + \Delta p_{skin}}{\bar{p} - p_{wf}}, \quad (1.22)$$

where J is the *productivity index* defined in Equation 1.12 and \bar{p} is the average pressure of the drainage area (in an infinite-acting reservoir, $\bar{p} = p_i$).

The *damage factor*:

$$DF = 1 - \frac{J_{actual}}{J_{ideal}} = \frac{-\Delta p_{skin}}{\bar{p} - p_{wf}} = 1 - FE. \quad (1.23)$$

Example 1.2

In Example 1.1, the measured bottom-hole pressure was

$$(p_{wf})_{real} = 30.82 \text{ MPa [4469 psi]}.$$

The following values are to be calculated:

- the skin factor

- the flow efficiency
- the borehole damage factor.

Solution:

The supplementary pressure loss caused by the skin is calculated by Equation 1.16:

$$\Delta p_{skin} = (p_{wf})_{real} - (p_{wf})_{ideal} = 30.82 - 32.64 = -1.82 \text{ MPa}.$$

In field units:

$$\Delta p_{skin} = 4469 - 4732 = -263 \text{ psi}.$$

The skin factor according to Equation 1.18 is:

$$s = \frac{\Delta p_{skin}}{\frac{q\mu B}{2\pi hk}} = \frac{-1.82 \times 10^6}{-0.746 \times 10^5} = 24.37.$$

In field units:

$$s = \frac{\Delta p_{skin}}{\frac{q\mu B}{0.00708 hk}} = \frac{-264}{-10.97} = 23.97.$$

The flow efficiency according to Equation 1.22 is:

$$\frac{J_{actual}}{J_{ideal}} = \frac{\bar{p} - p_{wf} + \Delta p_{skin}}{\bar{p} - p_{wf}} = \frac{33.24 - 30.82 - 1.82}{33.24 - 30.82} = \frac{0.60}{2.42} = 0.248 \cong 25\%.$$

In field units:

$$\frac{J_{actual}}{J_{ideal}} = \frac{4819.8 - 4469 - 264}{4819.8 - 4469} = 0.25 = 25\%.$$

The damage factor is 1 minus flow efficiency, i.e. 75%.

1.5. Principle of Superposition

The first and second theorem of superposition were discussed in "*Fluid Flow in Porous Media*"^[6], Chap. 3.2.2 and 3.2.3. This is only a short summary of the conclusions drawn there.

In Figure 1.10, the formation is produced with three wells. Well 1 begins production at $t_1 = 0$ at a constant rate q_1 , and causes a pressure decline in the observation well $\Delta p_{3,1}(t)$. Well 2 starts production later, at time t_2 . If well 2 was the only production well, the pressure change in well 3 would be $\Delta p_{3,2}(t - t_2)$.

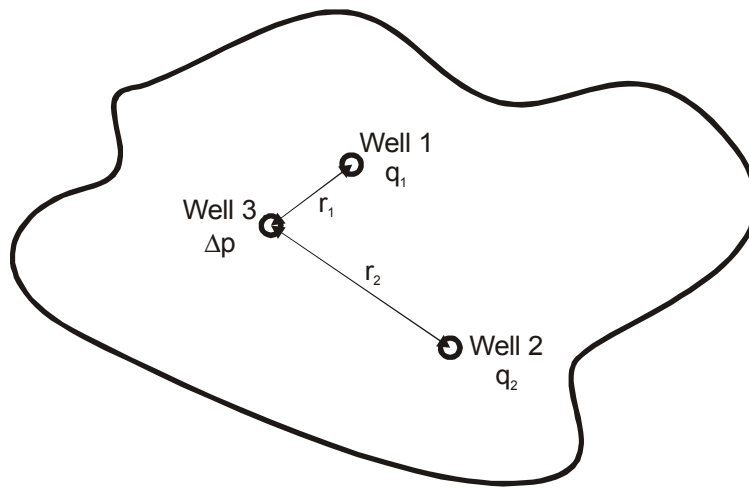


Figure 1.10: Infinitely acting reservoir with several wells

According to the principle of superposition (second theorem), if both wells produce, the pressure change can be calculated by adding these differences:

$$\Delta p_3 = \Delta p_{3,1} + \Delta p_{3,2} \quad (1.24)$$

By means of the dimensionless variables, Equation 1.25 can be written in the following way for any number of wells:

$$\Delta p(t, r) = \frac{\mu}{2\pi h k} \sum_{j=1}^n q_j B_j p_D(t_D - t_{Dj}, r_{Dj}), \quad (1.25)$$

where t_{Dj} are the dimensionless times of putting the individual wells into operation and r_{Dj} are the dimensionless distances of wells from the point of observation. If there is a producing well at this point, one has to add to Δp according to Equation 1.24 the pressure loss Δp_{skin} for this (and only for this) well.

Imagine that n wells ($j = 1, \dots, n$) are located at the same point, and each of them produces at a constant rate q_j beginning at time t_j . Equation 1.25 remains valid, we have only to substitute $r_{D1} = r_{D2} = \dots = r_{Dn} = 1$.

If "all wells" are at the same location, it is sufficient to regard only one well whose rate changes at the time t_{Dj} with Δq_j (this change can be positive or negative). The pressure change caused by one well producing at a varying rate can also be calculated by summarizing up the elementary pressure changes:

$$\Delta p(t, r) = \frac{\mu B}{2\pi h k} \sum_{j=1}^n \Delta q_j p_D(t_D - t_{Dj}, r_{Dj}). \quad (1.26)$$

With the skin effect, Equation 1.26 is written in the following way:

$$\Delta p(t, r) = \frac{\mu B}{2\pi h k} \left[\sum_{j=1}^n \Delta q_j p_D(t_D - t_{Dj}, r_{Dj}) + q_n s \right]. \quad (1.27)$$

Example 1.3

The rate of well $q_1 = -40 \text{ m}^3/d$ [251.6 bbl/d] in Example 1.1 and 1.2 is reduced after five days to $q = -25 \text{ m}^3/d$ [157.2 bbl/d]. The bottom-hole flowing pressure after 20 days is to be calculated.

Solution:

For the terms of Equation 1.26, there are:

$$\begin{aligned} t_1 &= 0 \\ t_2 &= 5 \text{ d} = 0.432 \times 10^6 \text{ s} \\ t &= 20 \text{ d} = 1.728 \times 10^6 \text{ s} \\ \Delta q_1 &= q_1 = -40 \text{ m}^3/d = -0.463 \times 10^{-3} \text{ m}^3/s \text{ [-251.5 bbl/d]} \\ \Delta q_2 &= q_2 - q_1 = 15 \text{ m}^3/d = 0.0174 \times 10^{-3} \text{ m}^3/s \text{ [94.33 bbl/d]} \\ q_2 &= -25 \text{ m}^3/d = -0.000289 \text{ m}^3/s \text{ [-157.23 bbl/d]} \end{aligned}$$

The dimensionless time differences according to Equation 1.2 are:

$$t_D - t_{D1} = \frac{k}{\phi \mu c_t r_w^2} (t - t_1) = 17.991 \times 1.728 \times 10^6 = 3.109 \times 10^7 \text{ [-]}$$

$$t_D - t_{D2} = 17.991 (1.728 - 0.432) \times 10^6 = 2.332 \times 10^7 \text{ [-]}$$

In field units:

$$t_D - t_{D1} = 20 \times 1.554 \times 10^6 = 3.108 \times 10^7 \text{ [-]},$$

$$t_D - t_{D2} = 1.554 \times 10^6 \times 15 = 2.331 \times 10^7 \text{ [-]}.$$

From Equation 1.8:

$$p_D(t_D - t_{D1}) = p_D(3.109 \times 10^7) = 8.94$$

$$p_D(t_D - t_{D2}) = p_D(2.332 \times 10^7) = 8.82$$

and the bottom hole flowing pressure after 20 days is:

$$\begin{aligned} p_{wf} &= p_i + \frac{\mu B}{2\pi h k} [\Delta q_1 p_D(t_D - t_{D1}) + \Delta q_2 p_D(t_D - t_{D2}) + q_2 s] \\ &= 33.24 \times 10^6 + \frac{1.28 \times 10^{-3} \times 1.52}{2\pi \times 12 \times 0.16 \times 10^{-12}} [-0.463 \times 10^{-3} \times 8.94 + \\ &\quad + 0.174 \times 10^{-3} \times 8.82 - 0.289 \times 10^{-3} \times 24.34] = 31.68 \text{ MPa}. \end{aligned}$$

In field units:

$$\begin{aligned} p_{wf} &= 4819.8 + 141.2 \times \frac{1.28 \times 1.52}{39.37 \times 160} \\ &\quad (-251.6 \times 8.94 + 94.55 \times 8.82 - 157.23 \times 23.97) = 4593.71 \text{ psi}. \end{aligned}$$

1.6. Wellbore Storage

In the mathematical model, the sandface flow is taken into account. It is equal to the production rate, measured at the well head, only if the well flow is steady-state. If the bottom-hole pressure changes - and this is always the case in hydrodynamic formation tests - the sandface flow is no longer equal to the production rate. If the bottom-hole pressure increases (decreases), the fluid content of the well increases (decreases) too. This after-production or after-injection should be

taken into consideration during the evaluation of the transient pressure change.

Ramey^[14] defined the wellbore storage constant in the following way:

$$C = \frac{\Delta G}{\rho \Delta p_w} \quad (1.28)$$

where

$$\begin{aligned} \Delta G & - \text{the fluid mass change in the well, } kg [lbm], \\ \rho & - \text{the fluid density in the well, } kg/m^3 [lbm/cu ft], \\ \Delta p_w & - \text{the bottom-hole pressure change, } Pa [psi]. \end{aligned}$$

This term can apply to filled up wells and to wells with free fluid level (see Example 1.4). Let q be the constant well rate and q_{sf} the sandface rate. Then

$$\Delta G = (q - q_{sf})B\rho\Delta t, \quad (1.29)$$

where B is the formation volume factor.

After the substitution of Equation 1.29 into Equation 1.28, we obtain

$$q - q_{sf} = \frac{C}{B} \frac{\Delta p_w}{\Delta t} = \frac{C}{B} \frac{dp_w}{dt}. \quad (1.30)$$

We now divide this equation by q and introduce the dimensionless variables defined in Equation 1.2 and Equation 1.4:

$$dt = \frac{\phi\mu c_t r_w^2}{k} dt_D, \quad (1.31)$$

$$dp_w = \frac{q\mu B}{2\pi hk} dp_{Dw}. \quad (1.32)$$

We get

$$1 - \frac{q_{sf}}{q} = \frac{C}{qB} \frac{\frac{q\mu B}{2\pi hk} dp_{Dw}}{\frac{\phi\mu c_t r_w^2}{k} dt_D} = \frac{C}{2\pi\phi c_t h r_w^2} \frac{dp_{Dw}}{dt_D}. \quad (1.33)$$

It is more convenient to apply a *dimensionless wellbore storage constant*:

$$C_D = \frac{C}{2\pi\phi c_t h r_w^2} \quad (1.34)$$

and write the Equation 1.33 in a shorter form:

$$C_D \frac{dp_{Dw}}{dt_D} = 1 - \frac{q_{sf}}{q}. \quad (1.35)$$

With field units, Equation 1.34 has the following form:

$$C_D = \frac{5.6146C}{2\pi\phi c_t h r_w^2}, \text{ where } C \text{ is given in bbl/psi.} \quad (1.36)$$

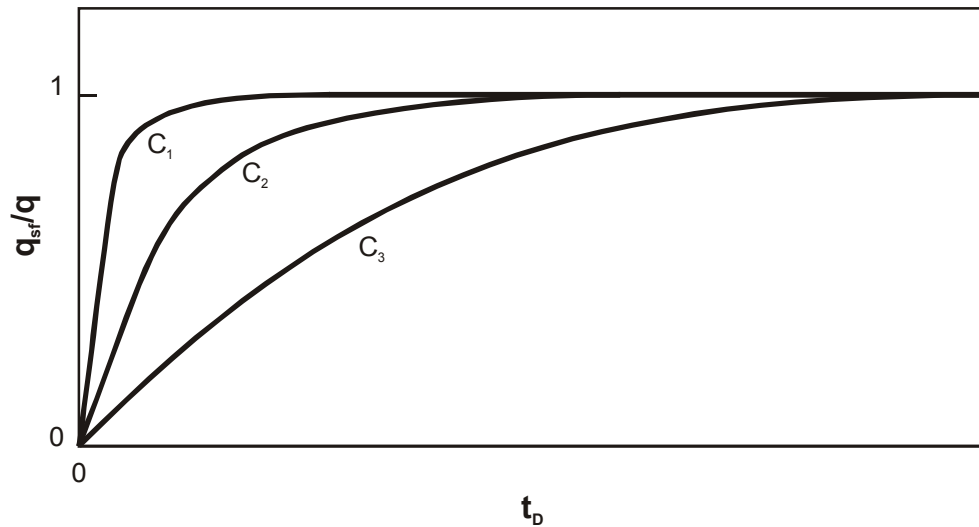


Figure 1.11: Effect of wellbore storage on sand face flow rate $C_3 > C_2 > C_1$

Figure 1.11 shows the ratio of sandface flow and production rate for that case where the production rate is constant. If $C = 0$, i.e. if there is no after-production, then $q_{sf} = q$ for any time.

Example 1.4

The tubings of the well in Example 1.1 have an internal volume of $V_u = 0.015 \text{ m}^3/\text{m}$ [$2.875 \times 10^{-2} \text{ bbl}/\text{ft}$] and a total length $L = 3125 \text{ m}$ [10252.6 ft]. The compressibility of the oil in the tubing is $c_o = 1.3 \times 10^{-9} \text{ Pa}^{-1}$ [$8.97 \times 10^{-6} \text{ 1}/\text{psi}$] and the density $\rho = 764 \text{ kgm}^{-3}$ [$47.7 \text{ lbm}/\text{cu ft}$]. The wellbore storage constant has to be determined.

Solution:

a) On the assumption that the well is filled up:

$$\Delta G = V_u L c_o \Delta p \rho_o$$

and from Equation 1.28:

$$C = V_u L c_o = 0.015 \times 3125 \times 1.3 \times 10^{-9} = 61 \times 10^{-9} \text{ m}^3 / \text{Pa}.$$

In field units:

$$C = V_u L c_o = 2.875 \times 10^{-2} \times 10252.6 \times 8.97 \times 10^{-6} = 2.664 \times 10^{-3} \text{ bbl/psi}.$$

The dimensionless wellbore storage coefficient from Equation 1.34:

$$C_D = \frac{C}{2\pi\phi c_t h r_w^2} = \frac{61 \times 10^{-9}}{2\pi \times 0.18 \times 3.86 \times 10^{-9} \times 12 \times 0.1^2} = 1.16 \times 10^2 [].$$

In field units:

$$C_D = \frac{2644 \times 10^{-3} \times 5.6146}{2\pi \times 0.18 \times 2.662 \times 10^{-5} \times 39.37 \times 0.328^2} = 1.17 \times 10^2 [].$$

b) On the assumption that the oil level rises:

A pressure increase of Δp means a rising of the oil level by

$$\Delta h = \frac{\Delta p}{\rho g},$$

therefore

$$\Delta G = V_u \Delta h \rho = V_u \frac{\Delta p}{g},$$

and

$$C = \frac{V_u}{\rho g} = \frac{0.015}{764 \times 9.81} = 2 \times 10^{-6} \text{ m}^3 / \text{Pa}.$$

In field units:

$$C = \frac{2.875 \times 10^{-2}}{47.7/144} = 8.679 \times 10^{-2} \text{ bbl/psi.}$$

The *dimensionless wellbore storage coefficient* is

$$C_D = \frac{C}{2\pi\phi c_t h r_w^2} = \frac{2 \times 10^{-6}}{2\pi \times 0.18 \times 3.86 \times 10^{-9} \times 12 \times 0.1^2} = 3817.76 \text{ [-].}$$

In field units:

$$C_D = \frac{8.679 \times 10^{-2} \times 5.6146}{2\pi \times 0.18 \times 2.662 \times 10^{-5} \times 39.37 \times 0.328^2} = 3821.33 \text{ [-].}$$

1.7. Pressure Change

The equations for the one-phase flow were derived in "*Fluid Flow in Porous Media*"^[6], Chapter 2. The solutions for idealized cases are given in Chapter 3. It sufficient to repeat the most important formulae here.

The pressure change caused by a well producing from an infinite acting, horizontal formation with relatively small thickness at a constant rate can be calculated with the following formula:

$$p_D(t_D, r_D) = -\frac{1}{2} Ei \left(-\frac{r_D^2}{4t_D} \right) \quad (1.37)$$

or

$$p_D(t_D, r_D) \cong \frac{1}{2} \left[\ln \left(t_D / r_D^2 \right) + 0.80907 \right], \quad (1.38)$$

where the approximation error of Equation 1.38 less then 1 % if

$$\frac{t_D}{r_D^2} > 10. \quad (1.39)$$

The solution for Equation 1.37 is shown in Figure 1.8. At the bottom-hole $r_D = 1$, therefore the condition represented by Equation 1.39 is practically always fulfilled, and Equation 1.38 is

simplified to:

$$p_D(t_D, r_D = 1) = \frac{1}{2}[\ln t_D + 0.80907], \quad (1.40)$$

or with consideration of the Equation 1.8:

$$p_{Dw}(t_D) = \frac{1}{2}[\ln t_D + 0.80907 + 2s]. \quad (1.41)$$

In the case of $C_D > 0$, where C_D is the dimensionless wellbore storage constant, Equation 1.41 can be written in the following form:

$$p_{Dw}(t_D) = 0.5[\ln(t_D/C_D) + 0.80907 + \ln(C_D e^{2s})]. \quad (1.42)$$

Note that Equation 1.41 and Equation 1.42 are identical. By splitting the \ln expressions C_D drops out. These equations are valid only if $q_{sf} = q$ and the wellbore volume has no influence on the bottom-hole pressure.

At the start of a well, the whole amount of fluid will be produced from the wellbore volume. That means, the sandface rate q_{sf} is zero at a small t_D . For this case we can write Equation 1.35 in the following form:

$$C_D \frac{dp_{Dw}}{dt_D} = 1, \quad (1.43)$$

or integrated, under consideration that $p_{Dw} = 0$ at $t_D = 0$,

$$p_{Dw} = \frac{t_D}{C_D}. \quad (1.44)$$

During the transition time, the sandface rate rises and converges to q . A dimensionless pressure $p_{Dw}(t_D)$ could theoretically be calculated for this period via superposition by using Equation 1.27.

Figure 1.8 shows the function Equation 1.37 in a log-log diagram. Figure 1.12 shows the same, but also taken into consideration are the skin and the wellbore storage effects. Equation 1.42 is valid only over the marked limit. All curves have a slope 1 for small t_D .

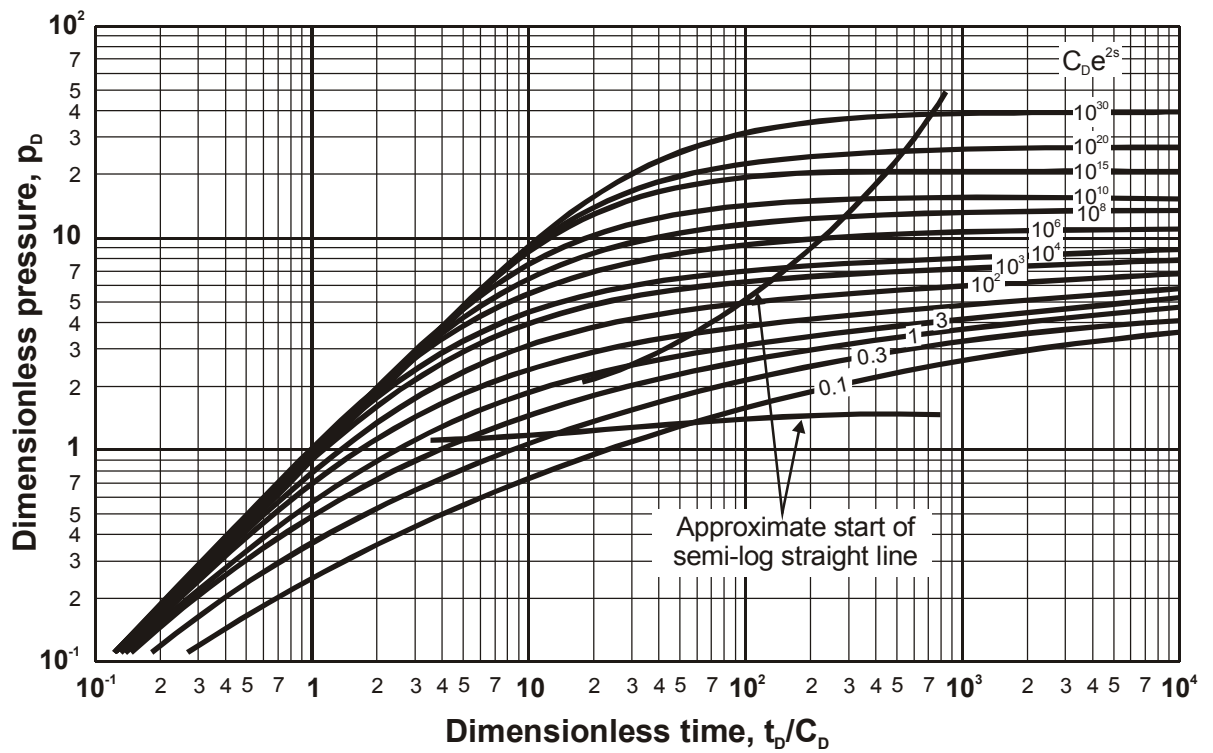


Figure 1.12: Type-curves for a single well inside a homogeneous reservoir with wellbore storage and skin effects (after BOURDET *et al.*^[2])

values. This is a consequence of Equation 1.44. Figure 1.13 is the same as the previous one, but the derivatives of the functions p_{Dw} are also drawn in the form

$$\frac{dp_{Dw}}{d(t_D/C_D)C_D} \frac{t_D}{C_D} \text{ vs. } \frac{t_D}{C_D}. \quad (1.45)$$

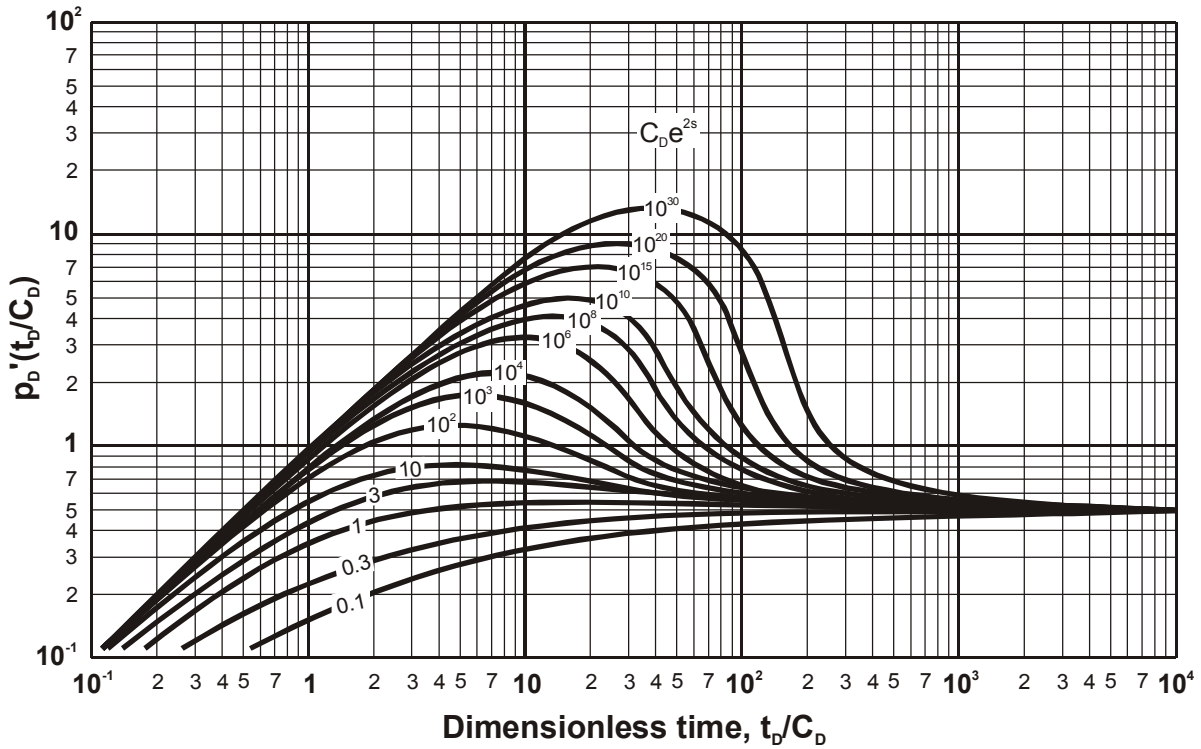


Figure 1.13: Log-log plot $p'_D \frac{t_D}{C_D}$ vs. $\frac{t_D}{C_D}$ (after BOURDET *et al.*[2])

In view of Equation 1.44, it follows that

$$\frac{dp_{Dw}}{d(t_D/C_D)} = p'_{Dw} = 1. \quad (1.46)$$

Hence the function $p_{Dw}(t_D/C_D)$ has the same slope of 1, as the function, p_{Dw} if t_D is small. Contrary to large t_D values all the functions $p_{Dw}(t_D/C_D)$ converge to

$$\frac{dp_{Dw}}{d(t_D/C_D)} = p'_{Dw} = 0.5/(t_D/C_D). \quad (1.47)$$

From the combination of Equation 1.9 and Equation 1.41 follows:

$$p_{wf}(t) = p_i + \frac{qB\mu}{4\pi hk} [\ln t_D + 0.80907 + 2s] = \quad (1.48)$$

$$= p_i + \frac{2.3026qB\mu}{4\pi hk} \left[\lg t + \lg \left(\frac{k}{\phi\mu c_l r_w^2} \right) + 0.35137 + 0.86859s \right]. \quad (1.49)$$

If the reservoir is not acting infinitely, but is bounded at a concentric circle r_{De} , then Equation

1.41 after van Everdingen and Hurst takes the following form:

$$p_{Dw}(t_D) = \frac{1}{2}[\ln t_D + 0.80907 + 2s + Y(t_D, r_{De})], \quad (1.50)$$

where,

$$Y(t_D, r_{De}) = -(\ln t_D + 0.80907) + \frac{4t_D}{r_{De}^2} + 2\left(\ln r_{De} - \frac{3}{4}\right) + 4 \sum \frac{e^{-\alpha_n^2 t_D} J_1(\alpha_n r_{De})}{\alpha_n^2 [J_1^2(\alpha_n r_{De}) - J_1^2(\alpha_n)]} \quad (1.51)$$

Equation 1.49 is modified correspondingly:

$$p_{wf}(t) = p_i + \frac{2.3026qB\mu}{4\pi hk} \times \left[\lg t + \lg \frac{k}{\phi \mu c_t r_w^2} + Y(t_D, r_{De}) + 0.35137 + 0.86859s \right]. \quad (1.52)$$

If t_D is small and the inflow radius is smaller than r_e then $Y(t_D, r_{De}) = 0$ and the function Equation 1.50 is equal to Equation 1.41. If t_D is large, then the last term of function Equation 1.51 disappears and

$$p_{Dw}(t_D) = \frac{2t_D}{r_{De}^2} + \ln r_{De} - \frac{3}{4} + s \quad (1.53)$$

or

$$p_{Dw}(t_{DA}) = 2\pi t_{DA} + \frac{1}{2} \ln \frac{A}{r_w^2} + \frac{1}{2} \ln \left(\frac{2.2458}{C_A} \right) + s, \quad (1.54)$$

where

$$\begin{aligned} A &= \pi r_{De}^2 && \text{the area of the reservoir,} \\ t_{DA} &= t_D (r_w^2 / A) && \text{(see Equation 1.3), and} \\ C_A &= 31.62 && \text{is a shape factor} \end{aligned}$$

The conversion into Equation 1.54 has the purpose to make the formula valid also for

non-circular finite formations. Only the shape factor C_A -as was shown by Ramey and Cobb^[15] - will be different. Table 1.1 indicates the shape factors and the validity limits of Equation 1.54.

Converting Equation 1.53 into dimensioned variable:

$$p_{wf} - p_i = \frac{qt}{\pi\phi c_t h r_e^2} + \frac{q\mu}{2\pi kh} \left[\ln \frac{r_e}{r_w} - \frac{3}{4} + s \right] \tag{1.55}$$

For production at constant rate, the average pressure in the reservoir is given by

$$\bar{p} = p_i + \frac{qt}{\pi\phi c_t h r_e^2} \tag{1.56}$$

Combining Equation 1.55 and Equation 1.56 and rearrange it, one obtains:

$$p_{wf} - \bar{p} = \frac{q\mu}{2\pi kh} \left(\ln \frac{r_e}{r_w} - \frac{3}{4} + s \right) \tag{1.57}$$

The p_D functions are presented in log-log diagrams, dependent on t_D , t_D/C_D or t_{DA} . Figure 1.8, Figure 1.13 and Figure 1.14 show a few examples. These curves are the so-called *type-curves*.

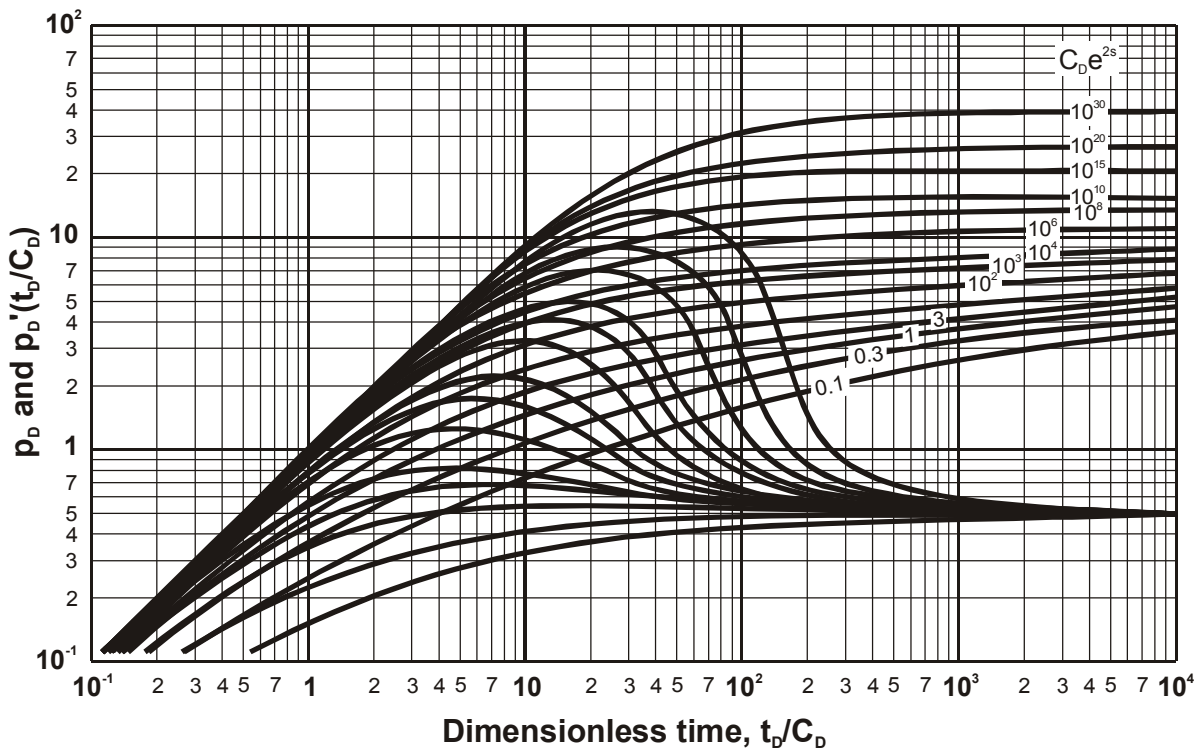


Figure 1.14: Type curves - homogenous reservoir with wellbore storage and skin (after

BOURDET *et al.*^[2])

1.7.1 Drainage Radius

The drainage radius r_D , i.e. the extension of a pressure funnel (cone) in an infinite acting formation, at the production time t can be estimated with the following formula:

$$r_d \cong 2 \sqrt{\frac{kt}{\phi\mu c_t}}; [m]. \quad (1.58)$$

For field units, the formula has to be written as

$$r_d = \left(\frac{kt}{948\phi\mu c_t} \right)^{0.5} \cong 0.0325 \sqrt{\frac{kt}{\phi\mu c_t}}; [ft]. \quad (1.59)$$

For a bounded formation with symmetrical shape and with the well in its center, the transient period will change into the pseudo-steady-state period when the radius r_D has reached the boundary. For a cylindrical reservoir with $A = r_d^2\pi$, the stabilization time from Equation 1.58 is the following:

$$t_s \approx 0.25 \frac{\phi\mu c_t r_d^2}{k}; [s] \quad (1.60)$$

or in field units

$$t_s \approx 948 \frac{\phi\mu c_t r_d^2}{k}; [hrs]. \quad (1.61)$$

If the shape of the drainage area is a square rather than a circle it takes longer to reach the pseudo-steady-state period:

$$t_s \approx 1200 \frac{\phi\mu c_t r_d^2}{k} \quad (1.62)$$

1.7.2 Multi-Phase Filtration

Below the bubble point, the gas dissolves in the reservoir, and therefore the one-phase filtration equations are, strictly speaking, not applicable. However, they may be used for multiple-phase flow situations with some modifications (see MILLER *et al.*^[12], PERRINE^[13], MARTIN^[9]).

Neglecting the capillary forces the equations describe the multi-phase filtration in a precise way, if the total compressibility c_t and the total mobility $(k/\mu)_t$ are substituted:

$$c_t = c_\phi + S_o c_{oa} + S_w c_w + S_g c_g, \quad (1.63)$$

$$\left(\frac{k}{\mu}\right)_t = k \left(\frac{k_{ro}}{\mu_o} + \frac{k_{rg}}{\mu_g} + \frac{k_{rw}}{\mu_w} \right). \quad (1.64)$$

The *apparent two phase compressibility for saturated oil* is

$$c_{oa} = -\frac{1}{B_o} \frac{\partial B_o}{\partial p} + \frac{B_g}{B_o} \frac{\partial R_s}{\partial p}. \quad (1.65)$$

This provides for the practical advantage that the evaluation of formation tests can be performed in the case of multi-phase filtration in the same way as for single-phase filtration.

1.7.3 Equations for Gas-Flow

The viscosity and especially the density of the gas change vary significantly with pressure. Therefore the filtration equation of the gas is not linear. This difficulty can be overcome by introducing the *real gas pseudo pressure* according to AL-HUSSAINY, RAMEY and CRAWFORD^[1].

$$m(p) = 2 \int_{p_b}^p \frac{p}{\mu(p)Z(p)} dp \quad (1.66)$$











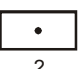
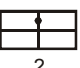
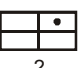
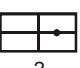
where p_b is a freely chosen reference pressure. By applying $m(p)$, the filtration equation of the gas becomes formally equal to that of the low-compressible fluids. In this case, Equation 1.9 changes into the following form (for SI units):

$$m(p_i) - m(p_{wf}) = 55.956 \frac{q_{sc} T}{hk} \left[\ln \frac{k}{\phi \mu_g c_g r_w^2} t + 0.809 + 2S + 2D|q_{sc}| \right]. \quad (1.67)$$

The term $D|q|$ is the dimensionless pressure drop caused by the turbulence in the well environment. The rate dependent skin coefficient has the dimensions s/m^3 for SI units.

After the introduction of the function $m(p)$, it is sufficient to discuss the liquid case. All procedures can be adapted for gas-bearing formations by means of this modification.

Table 1.1: Shape Factors for Bounded Drainage Areas (after RAMEY and COBB^[15])

in bounded reservoirs	C_A	$\ln C_A$	$1/2 \ln C_A \left(\frac{2.2458}{C_A} \right)$	exact for $t_{DA}^>$	less than 1% error for $t_{DA}^>$	use infinite system solution with less than 1% error for $t_{DA}^<$
	31.62	3.4538	-1.3224	0.1	0.06	0.100
	31.6	3.4532	-1.3220	0.1	0.06	0.100
	27.6	3.3178	-1.2544	0.2	0.07	0.090
	27.1	3.2995	-1.2452	0.2	0.07	0.090
	21.9	3.0865	-1.1387	0.4	0.12	0.080
	0.098	-2.3227	+1.5659	0.9	0.60	0.015
	30.8828	3.4302	-1.3106	0.1	0.05	0.090
	12.9851	2.5638	-0.8774	0.7	0.25	0.030
	4.5132	1.5070	-0.3490	0.6	0.30	0.025
	3.3351	1.2045	-0.1977	0.7	0.25	0.010
	21.8369	3.0836	-1.1373	0.3	0.15	0.025
	10.8374	2.3830	-0.7870	0.4	0.15	0.025
	4.5141	1.5072	-0.3491	1.5	0.50	0.060
	2.0769	0.7309	+0.0391	1.7	0.50	0.020

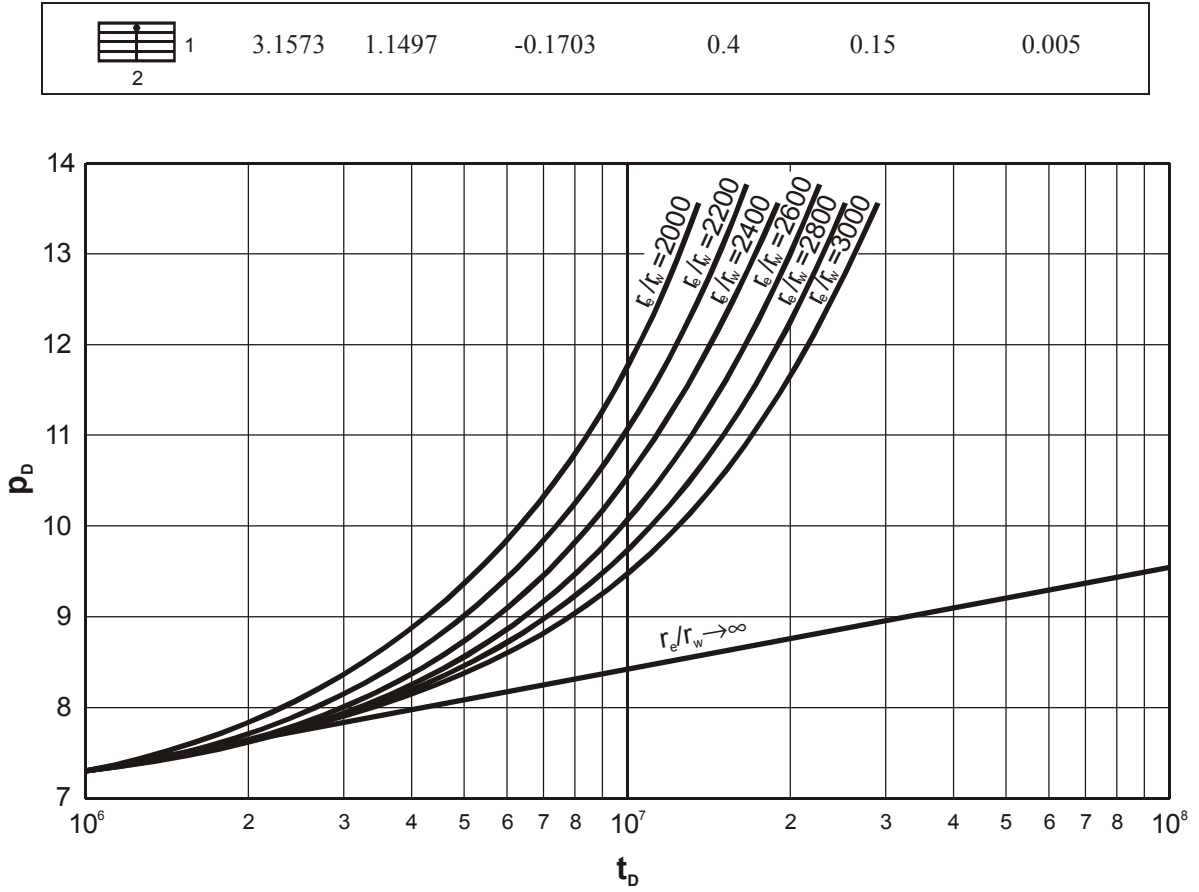


Figure 1.15: Dimensionless pressure for a well in the center of a closed circular reservoir, no wellbore storage, no skin (EARLOUGHER and RAMEY^[5])

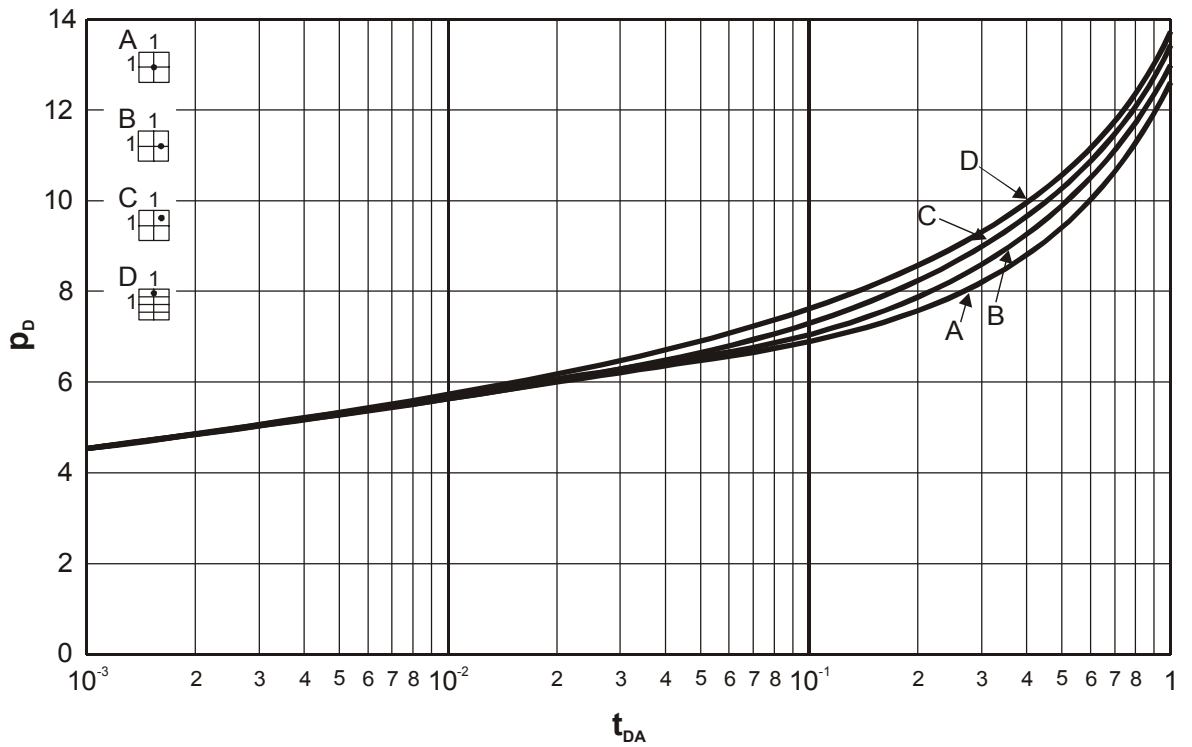


Figure 1.16: Dimensionless pressure for a single well in various closed rectangular systems, no wellbore storage, no skin (EARLOUGHER and RAMEY^[5])

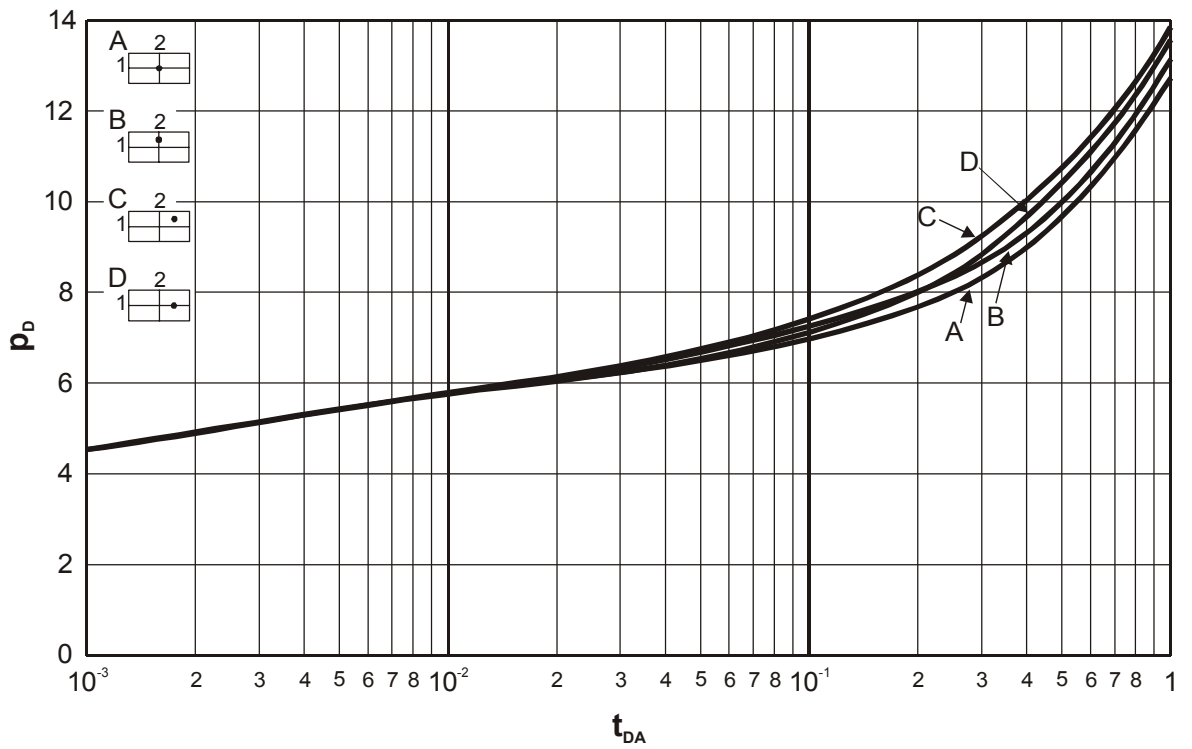


Figure 1.17: Dimensionless pressure for a single well in various closed rectangular systems, no wellbore storage, no skin (EARLOUGHER and RAMEY^[5])

2 Pressure Drawdown Analysis

2.1. Semilog Plot

A well is put into operation at the time $t = 0$ at a constant production rate. The bottom-hole pressure change is shown in Figure 1.1. Two parts of this curve are especially significant: the transient period and the pseudo-steady state period.

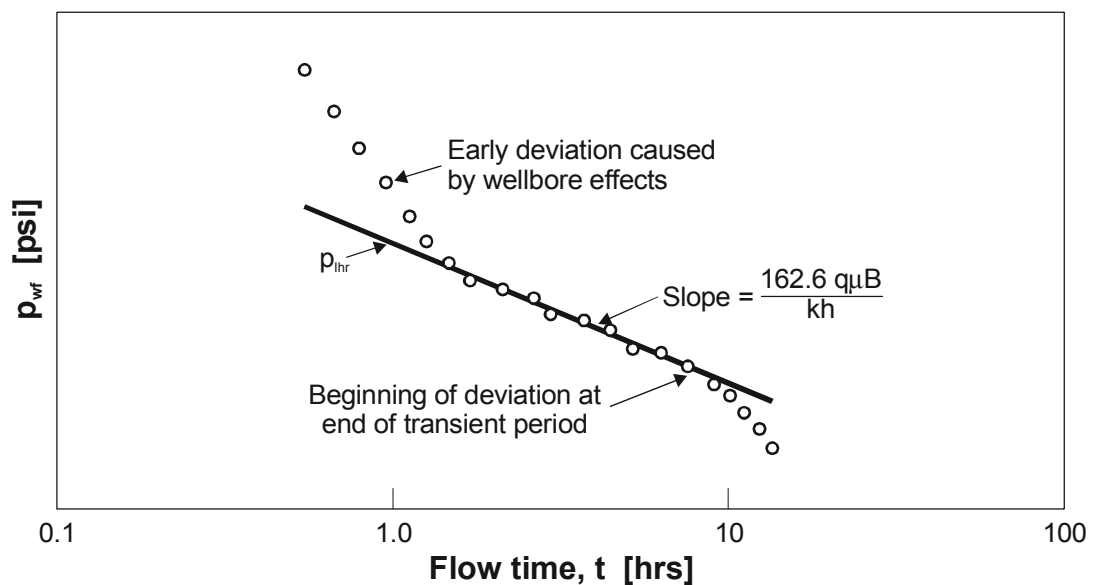


Figure 2.1: Evaluation of the transient pressure drop (after MATTHEWS and RUSSEL^[11])

Figure 2.1 shows this curve vs. $\lg t$. During transient period ($t < t_s$), the drainage radius has not reached the external boundary yet, therefore the formation can be considered as infinite and Equation 1.49 is valid. The bottom-hole pressure p_{wf} is a linear function of $\lg t$. If the measured points allow a reliable drawing of a straight line, the permeability capacity of the formation hk can be calculated from the slope of the line. From Equation 1.49:

$$m = \left(\frac{2.3026}{4\pi} \right) \frac{q\mu B}{hk} \quad (2.1)$$

and

$$hk = 0.183 \frac{q\mu B}{m} \quad (2.2)$$

In field units, Equation 2.2 is written as

$$hk = 162.6 \frac{q\mu B}{m}. \quad (2.3)$$

From the pressure drawdown curve the skin effect can also be calculated, provided that the initial pressure is known. From the straight line one reads the value p_{wf} at t_1 , and from Equation 1.49:

$$s = -1.1513 \left[\frac{p_i - p_{wf}(t_1)}{m} + \lg t_1 + \lg \left(\frac{k}{\phi \mu c_t r_w^2} \right) + 0.35137 \right]. \quad (2.4)$$

In field units

$$s = -1.1513 \left[\frac{p_i - p_{wf}(t_1)}{m} + \lg t_1 + \lg \left(\frac{k}{\phi \mu c_t r_w^2} \right) - 3.2275 \right]. \quad (2.5)$$

In the case of small time values, the measured points deviate from the straight line because of after-production. If the production time is not long enough, there is no possibility for the *semilog* evaluation. Here the *method of type curve matching* can be applied.

2.2. Type Curve Matching

This method is applicable for all transient measurements (pressure drawdown, pressure buildup, interference, pulse test) if the $p_D(t_D)$ -function is known for the given case.

Type curve matching is based on the fact that if the same events are represented in the log-log coordinate system with the variables p_D vs. t_D/C_D and $\Delta p = p - p_i$ vs. t the two curves will be shifted apart from each other, but otherwise will be the same. This statement is caused by the coordinates transformation Equation 1.2 and Equation 1.4. The shifting of log-log coordinate systems can be calculated immediately from these equations.

$$\lg(t_D/C_D) = \lg t + \lg \left(\frac{k}{\phi \mu c_t r_w^2} \right) - \lg \left(\frac{C}{2\pi \phi \mu c_t h r_w^2} \right) = \lg t - \lg \left(\frac{C\mu}{2\pi h k} \right), \quad (2.6)$$

$$\lg p_D = \lg |p - p_i| + \lg \left(-\frac{2\pi h k}{q\mu B} \right). \quad (2.7)$$

Type curve matching consists of the following steps:

- a.) Selection of the type curve diagram (sheet A). In this case it is Figure 1.14.
- b.) A transparent sheet of paper (sheet B) is positioned on the type curve diagram, and the coordinate lines are drawn. In this way it is provided that both systems of

coordinates are identical.

- c.) The measured Δp -values and the derivatives $\Delta p/t$ are drawn vs. t on sheet B.
- d.) By parallel shifting this series of points is adapted to one of the type curves.
- e.) After the successful adaptation, a reference point is selected, i.e. the *Match Point*. Its coordinates on sheet A and sheet B are

$$(p_D)_M, (t_D/C_D)_M \text{ and } \Delta p_M t_M.$$

At the same time also the value of $C_D e^{2s}$ can be determined.

- f.) From Equation 2.7 follows

$$k = \frac{q\mu_B (p_D)_M}{2\pi h (\Delta p)_M}. \quad (2.8)$$

- g.) The wellbore storage constant can be calculated from Equation 2.6:

$$C = \frac{2\pi h k t_M}{\mu (t_D/C_D)_M}. \quad (2.9)$$

Therefore,

$$C_D = \frac{C}{2\pi\phi c_t h r_w^2}. \quad (2.10)$$

- h.) The skin factor is defined by

$$s = 0.5 \ln[(C_D e^{2s}/C_D)]. \quad (2.11)$$

Type curve matching is less reliable than semilog evaluation and should only be applied if the latter method is not usable. In field units Equation 2.8 and Equation 2.10 are:

$$k = 141.2 \frac{q\mu_B (p_D)_M}{h (\Delta p)_M}, \quad (2.12)$$

$$C_D = \frac{5.6416 \times C}{2\pi\phi c_t h r_w^2} = \frac{0.8936 \times C}{\phi c_t h r_w^2}. \quad (2.13)$$

2.3. Reservoir Limit Testing

If the reservoir is bounded and the production time is sufficiently long, then Equation 1.54 will describe the pressure change:

$$p_{Dw}(t_D) = 2\pi t_{DA} + \frac{1}{2} \ln\left(\frac{A}{r_w^2}\right) + \frac{1}{2} \ln\left(\frac{2.2458}{C_A}\right),$$

or with dimensioned variables according to Equation 1.3 and Equation 1.4:

$$p_{wf} = m^*t + b, \quad (2.14)$$

where

$$m^* = \frac{qB}{\phi c_t h A}, \quad (2.15)$$

$$b = p_i + \frac{q\mu B}{4\pi h k} \left[\ln\left(\frac{A}{r_w^2}\right) + \ln\left(\frac{2.2458}{C_A}\right) + 2s \right]. \quad (2.16)$$

The measured p_{wf} -values are drawn as function of t , and a straight line is positioned along these points. From the slope m^* , the pore volume of the reservoir can be calculated:

$$\phi h A = \frac{qB}{c_t m^*}. \quad (2.17)$$

In field units:

$$\phi h A = 5.37 \times 10^{-6} \frac{qB}{c_t m^*}. \quad (2.18)$$

Theoretically, the shape factor C_A could also be determined from b , but the unreliability is so great that it should not be done.

Example 2.1

A pressure drawdown test was carried out in an undersaturated oil reservoir. The data and results are the following:

$$\begin{aligned} p_i &= 20.7 \text{ MPa [3002.3 psi]} \\ B_{oi} &= 1.32 [] \\ \mu_o &= 9.2 \times 10^{-3} \text{ Pas [9.2 cp]} \\ h &= 21 \text{ m [68.9 ft]} \\ \phi &= 0.17 [] \\ S_{wi} &= 0.26 [] \\ c_t &= 1.2 \times 10^{-9} \text{ Pa}^{-1} [8.27 \times 10^{-6} \text{ 1/psi}] \end{aligned}$$

$$\begin{aligned}
 p_i &= 20.7 \text{ MPa} [3002.3 \text{ psi}] \\
 r_w &= 0.1 \text{ m} [0.328 \text{ ft}] \\
 q &= -17.2 \text{ m}^3/\text{d} [108.2 \text{ bbl/d}]
 \end{aligned}$$

On the basis of the transient pressure development, the following values are to be determined:

- the permeability,
- the skin effect,
- the wellbore storage constant.

Solution:

a.) Semilog analysis

The measured pressure values are applied in Figure 2.2 to the semilog coordinate sheet.

The gradient is

$$m = \frac{\Delta p}{\text{cycle}} = -2.72 \times 10^5 \text{ Pa/cycle} = [-39.44 \text{ psi/cycle}]$$

and the extrapolation of the straight line give at $t_1 = 10 \text{ hour}$ the pressure $p_{wf} = 18.54 \text{ MPa} [2688.3 \text{ psi}]$.

From Equation 2.2,

$$k = 0.183 \frac{q\mu B}{hm} = 0.183 \frac{-17.2 \times 1.32 \times 9.2 \times 10^{-3}}{86400(-2.72) \times 10^5 \times 21} = 0.074 \times 10^{-12} \text{ m}^2.$$

From Equation 2.4, the skin effect is

$$\begin{aligned}
 s &= -1.1513 \left[\frac{p_i - p_{wf}(t_1)}{m} + \lg t_1 + \lg \frac{k}{\phi \mu c_t r_w^2} + 0.35173 \right] \\
 s &= -1.1513 \left[\frac{(20.7 - 18.54) \times 10^6}{-0.27 \times 10^5} + \lg 36000 + \right. \\
 &\quad \left. + \lg \left(\frac{0.074 \times 10^{-12}}{0.17 \times 9.2 \times 10^{-3} \times 1.2 \times 10^{-9} \times 0.1^2} \right) + 0.35137 \right] \\
 s &= (-1.1513[-7.94 + 4.56 + 0.595 + 0.35173]) = 2.8.
 \end{aligned}$$

In field units:

$$k = 162.9 \frac{q\mu B}{hm} = 162.9 \frac{-108.2 \times 1.32 \times 9.2}{-39.44 \times 68.9} = 78.7 \text{ mD},$$

$$s = -1.1513 \left[\frac{3001.5 - 2688.3}{-39.44} + \lg 10 + \lg \left(\frac{78.5}{0.17 \times 9.2 \times 8.27 \times 10^{-6} \times 0.328^2} \right) - 3.2275 \right]$$

$$s = -1.1513 [-7.96 + 1.0 + 7.7514 - 3.2275] = 2.8.$$

b.) Type curve matching method

In Figure 2.2, the measured pressure differences Δp and the product $\Delta p't$, depending on t , are applied to transparent log-log diagrams and matched by parallel shifting with curves in Figure 1.15.

The matched curve corresponds to $C_D e^{2s} = 10^8$.

We choose the match point:

$$\begin{aligned} p_{DM} &= 5.6 \\ (t_D/C_D)_M &= 3.4 \\ \Delta p_M &= 1 \text{ MPa [145 psi]} \\ t_M &= 1 \text{ hour} \end{aligned}$$

Using Equation 2.8 - Equation 2.11,

$$k = \frac{p_{DM} q \mu B}{\Delta p_M 2\pi h} = \frac{5.6 \times 17.2 \times 9.2 \times 10^3 \times 1.32}{1 \times 10^6 \times 86400 \times 2\pi \times 21} = 0.1026 \times 10^{-12} \text{ m}^2,$$

$$C = \frac{2\pi h k}{\mu (t_D/C_D)_M} = \frac{2\pi \times 0.1026 \times 10^{-12} \times 21 \times 3600}{9.2 \times 10^{-3} \times 3.4} = 1.558 \times 10^{-6} \text{ m}^3/\text{Pa} \cong 0.06756 \text{ bbl/psi},$$

$$C_D = \frac{C}{2\pi \phi c_t r_w^2 h} = \frac{1.558 \times 10^{-6}}{2\pi \times 0.17 \times 1.2 \times 10^{-9} \times 0.1^2 \times 21} = 5788.6,$$

$$s = 0.5 \ln \frac{C_D e^{2s}}{C_D} = 0.5 \ln \frac{10^8}{C_D} = 4.8.$$

In field units:

$$C_D = \frac{0.8936 C}{\phi c_t h r_w^2} = \frac{0.8936 \cdot 0.06756}{0.17 \cdot 8.25 \cdot 10^{-6} \cdot 68.9 \cdot 0.328^2} = 5793.1$$

$$s = 0.5 \ln \frac{10^8}{C_D} = 4.87$$

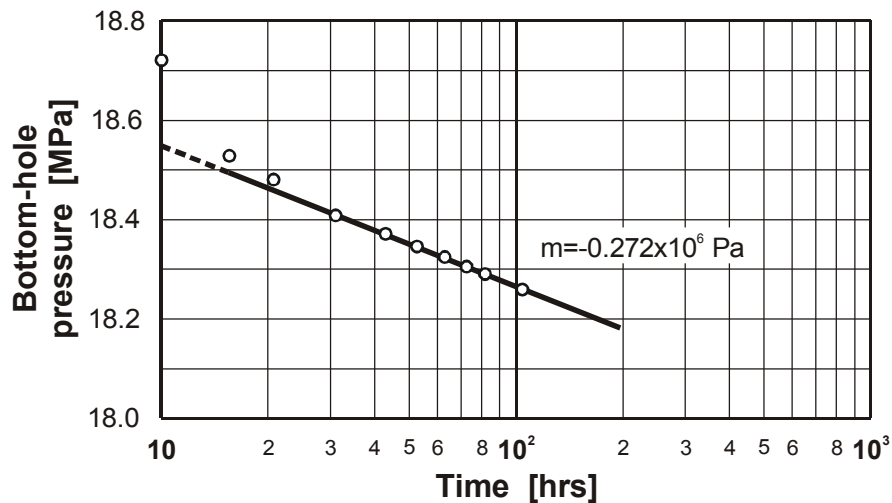


Figure 2.2: Semilog plot of pressure drawdown data

Example 2.2

From the pressure drawdown measurement in Example 2.1, the pore volume and the original oil in place (OOIP) are to be determined.

Solution:

In Figure 2.3, the measured bottom-hole pressure for $t > 100$ hours, depending on t , are drawn. The slope of the straight line is

$$m^* = -0.0508 \times 10^5 \text{ Pa/hour} = -1.41 \text{ Pa s}^{-1} = -0.7366 \text{ psi/h}.$$

From Figure 2.16:

$$\phi h A = \frac{qB}{c_t m^*} = \frac{-17.2 \times 1.32}{86400 \times 1.2 \times 10^{-9} (-1.41)} = 1.55 \times 10^5 \text{ pm}^3.$$

The OOIP:

$$N = \frac{\phi h A (1 - S_{wi})}{B_{oi}} = \frac{1.55 \times 10^5 (1 - 0.26)}{1.32} = 87.1 \times 10^3 \text{ m}^3.$$

In field units:

$$\phi hA = 5.37 \times 10^{-6} \frac{-108.2 \times 1.32}{8.27 \times 10^{-6} \times (-0.7366)} = 126 \text{ ac ft},$$

$$N = 7758 \frac{\phi hA(1 - S_{wi})}{B_{oi}} = \frac{7758 \times 126 \times (1 - 0.26)}{1.32} = 5.47 \times 10^5 \text{ bbl}.$$

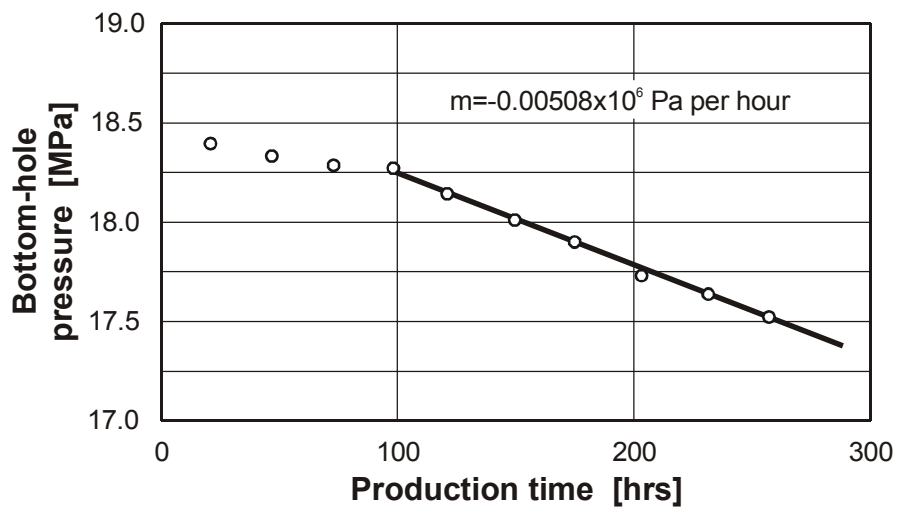


Figure 2.3: Reservoir limit testing for pressure drawdown data

Table 2.1: Pressure Decline

Time hour	Bottom Hole Pressure		$\Delta p = p_i - p_{wf}$		$\Delta p' t$	
	$10^5 Pa$	[psi]	$10^5 Pa$	[psi]	$10^5 Pa$	[psi]
0	207.00	3001.5				
1	201.35	2919.6	5.65	81.9	5.60	81.2
2	197.80	2868.1	9.20	133.4	6.50	94.3
3	195.35	2826.8	12.05	174.7	7.20	104.4
4	193.80	2810.1	13.20	191.4	7.30	105.9
5	192.00	2784.0	15.00	217.5	7.00	101.5
6	190.88	2767.7	16.12	233.7	6.60	95.7
7	189.90	2753.5	17.10	247.9	5.90	85.6
8	188.95	2727.4	18.05	261.7	5.00	72.5
9	188.08	2737.6	18.92	274.3	4.60	66.7
10	187.20	2714.4	19.80	287.1	4.20	60.9
15	185.30	2686.8	21.70	314.6	2.50	36.3
20	184.75	2678.9	22.25	322.6	1.70	24.7
30	184.10	2669.4	22.90	332.0	1.30	18.9
40	183.16	2664.5	23.24	337.0	1.26	18.3
50	183.47	2660.3	23.53	344.2	1.20	17.4
60	183.25	2657.1	23.75	344.4	1.15	16.7
70	183.08	2654.7	23.92	346.8	1.10	16.0
80	182.91	2652.2	24.09	349.3	1.02	14.8
100	182.70	2649.1	24.30	352.0	1.01	14.6
120	181.40	2630.3	25.60	371.0	0.00	14.5
***	***.**	****.*	**.**	***.*	***	***.*
144	180.22	2613.2	26.78	388.3		
168	179.00	2595.5	28.00	406.0		
192	177.75	2577.3	29.25	424.1		
216	176.59	2560.6	30.41	440.9		
240	175.30	2541.8	31.70	459.6		

3 Pressure Build Up Curve

A well produces at constant rate during a time period t_p . Then it is shut in. Figure 1.5 shows the bottom hole pressure curve. The pressure development for the time Δt after shut in can be calculated by means of the superposition principle. By this method, the pressure buildup caused by an injection rate q starting at time t_p will be superposed on the pressure decline caused by a continuous production at a rate q . By using Equation 1.27,

$$p_{ws} - p_i = \frac{q\mu B}{2\pi hk} [p_{Dw}([t_p + \Delta t]_D) - p_{Dw}(\Delta t_D)]. \quad (3.1)$$

After substituting of Equation 1.50,

$$\begin{aligned} p_{ws} &= p_i + \frac{q\mu B}{4\pi hk} [\ln[t_p + \Delta t]_D + 0.80907 + Y([t_p + \Delta t]_D, r_{De}) \\ &\quad - \ln \Delta t_D - 0.80907 - Y(\Delta t_D, r_{De})] \\ &= p_i + \frac{q\mu B}{4\pi hk} \left[\ln \left(\frac{t_p + \Delta t}{\Delta t} \right) + Y([t_p + \Delta t]_D, r_{De}) - Y(\Delta t_D, r_{De}) \right]. \end{aligned} \quad (3.2)$$

3.1. Horner Plot

This method for evaluation pressure buildup test was introduced by HORNER (1951). If the reservoir is sufficiently large and the shut in time is short, from Equation 1.51 it follows that

$$\begin{aligned} Y([t_p + \Delta t]_D, r_{De}) &\approx Y(t_{Dp}, r_{De}), \\ Y(\Delta t_D, r_{De}) &\equiv 0, \end{aligned} \quad (3.3)$$

and Equation 3.2 yields the following form:

$$p_{ws} = p_i + \frac{q\mu B}{4\pi hk} \left[\ln \frac{t_p + \Delta t}{\Delta t} + Y(t_{Dp}, r_{De}) \right] \quad (3.4)$$

$$\begin{aligned} &= \frac{2.3026 q\mu B}{4\pi hk} \lg \frac{t_p + \Delta t}{\Delta t} + p_i + \frac{q\mu B}{4\pi hk} Y(t_{Dp}, r_{De}) \\ &= 0.183 \frac{q\mu B}{hk} \lg \frac{t_p + \Delta t}{\Delta t} + p_i + \frac{0.183 q\mu B}{2.3026 hk} Y(t_{Dp}, r_{De}) \end{aligned} \quad (3.5)$$

$$= m \lg \frac{t_p + \Delta t}{\Delta t} + p_i + \frac{m}{2.3026} Y(t_{Dp}, r_{De}) \quad (3.6)$$

$$= m \lg \frac{t_p + \Delta t}{\Delta t} + p^* \tag{3.7}$$

Figure 3.1 shows a measured pressure buildup curve as a function of $\lg[(t_p + \Delta t)/\Delta t]$. The slope of the straight part, according to Equation 3.7 is

$$m = \frac{\Delta p}{\text{Cycle}} = 0.183 \frac{q\mu B}{hk} \tag{3.8}$$

From this,

$$hk = 0.183 \frac{q\mu B}{m} \tag{3.9}$$

In field units:

$$hk = 162.6 \frac{q\mu B}{m} \tag{3.10}$$

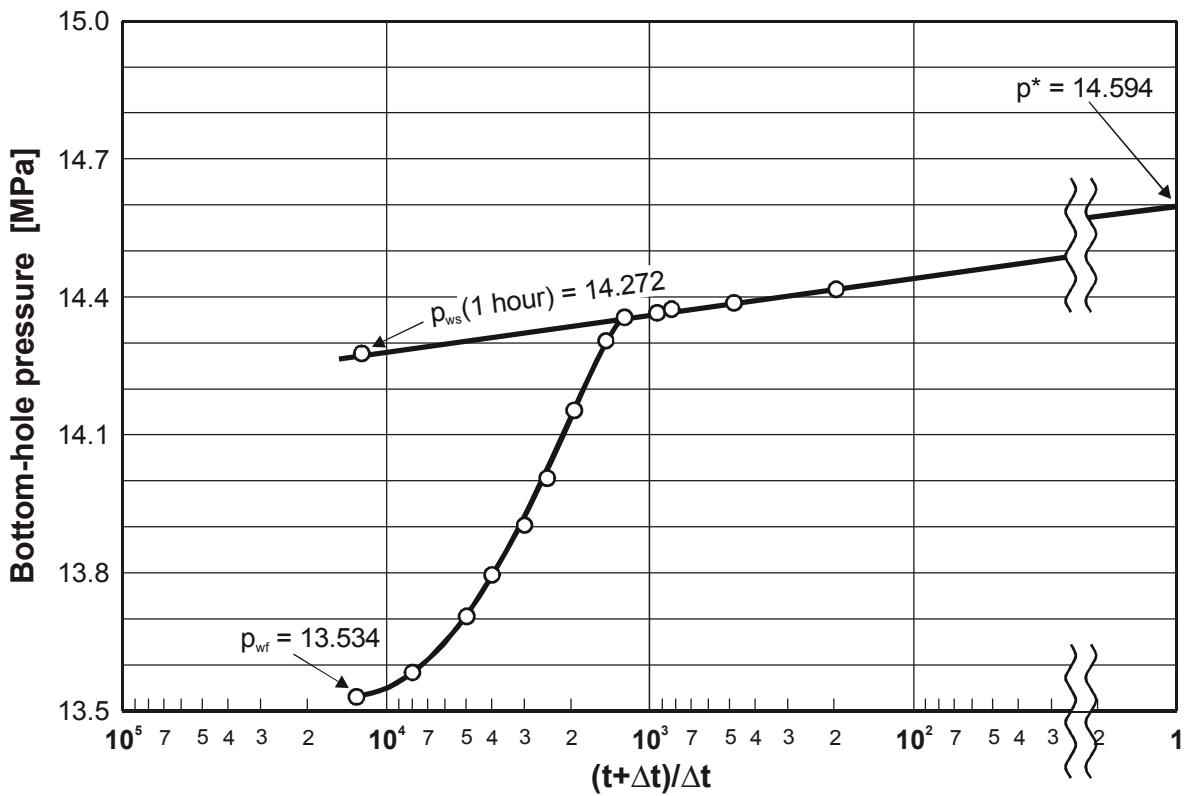


Figure 3.1: Pressure buildup curve with skin effect and wellbore storage

3.2. Type Curve Matching

Pressure buildup curves can also be evaluated by *type curve matching* and the same *type curves* as for the pressure drawdown analysis are used. We plot:

$$(i) \Delta p_{ws} = p_{ws}(\Delta t) - p_{wf}(t_p) \text{ vs } \Delta t$$

$$(ii) p'_{ws} \Delta t \frac{t_p + \Delta t}{t_p} \text{ vs } \Delta t$$

The reason for that can be shown in the following way. From Equation 1.4,

$$p_{wf}(t_p) - p_i = \frac{q\mu B}{2\pi hk} p_{Dw}(t_{Dp}). \quad (3.11)$$

After subtraction of this equation from Equation 3.1, we get

$$\Delta p_{ws} = -\frac{q\mu B}{2\pi hk} [p_{Dw}(\Delta t_D) + p_{Dw}(t_{Dp}) - p_{Dw}([t_p + \Delta t]_D)] \quad (3.12)$$

or

$$\Delta p_{Dws}(\Delta t_D) = p_{Dw}(\Delta t_D) + p_{Dw}(t_{Dp}) - p_{Dw}([t_p + \Delta t]_D). \quad (3.13)$$

In the case of

$$p_{Dw}(t_{Dp}) - p_{Dw}([t_p + \Delta t]_D) \ll p_{Dw}(\Delta t_D), \quad (3.14)$$

Equation 3.12 can be reduced to the form

$$-\Delta p_{Dws}(\Delta t_D) = p_{Dw}(\Delta t_D), \quad (3.15)$$

where p_{Dw} will be calculated by Equation 1.43. The requirement in Equation 3.14 is met if t_p is long and Δt is short.

Just after shut in (for very small Δt), the sandface flow rate q_{sf} is equal to the last well rate, notified with q . The actual well rate is now zero. Equation 3.13 becomes

$$-\Delta p_{Dws} = 0.5 \left[\ln \frac{\Delta t_D}{C_D} + \ln \frac{t_{pD}}{C_D} + \ln \frac{(t_p + \Delta t)_D}{C_D} + 0.80907 - \ln(C_D e^{2s}) \right]. \quad (3.16)$$

Derivative to respect $\Delta t_D / C_D$:

$$-\Delta p'_{Dws} = 0.5/(\Delta t_D/C_D) - 0.5/((t_p + \Delta t)_D/C_D) = 0.5 \frac{t_{pD}}{t_{pD} + \Delta t_D} / \frac{\Delta t_D}{C_D}, \quad (3.17)$$

or after reordering,

$$-\frac{t_{pD} + \Delta t_D}{t_{pD}} \frac{\Delta t_D}{C_D} \Delta p'_{Dws} = 0.5. \quad (3.18)$$

3.3. Skin Factor

From the pressure buildup curve, the skin factor can also be determined. If the well were closed at the bottom, the Δp_{skin} pressure difference would have to disappear at once and the curve would have to follow Equation 1.52 during this short time:

$$p_{wf} = p_i + 0.183 \left[\frac{q\mu B}{hk} + \lg(t_p + \Delta t) \lg \left(\frac{k}{\phi\mu c_t r_w^2} \right) + 0.35137 + Y([t_p + \Delta t]_D, r_{De}) + 0.86859s \right]. \quad (3.19)$$

If Equation 3.19 is subtracted from Equation 3.5 and if it is taken into consideration that $Y(tp + \Delta p_D, r_{De}) = Y(t_{Dp}, r_{De})$, then

$$p_{ws} - p_{wf} = -0.183 \frac{q\mu B}{hk} \left[\lg \Delta t + \lg \left(\frac{k}{\phi\mu c_t r_w^2} \right) + 0.35137 + 0.86859s \right]. \quad (3.20)$$

If one substitutes $\Delta t = 1 \text{ s}$, it follows from Equation 3.20 that

$$s = -1.1513 \left[\frac{p_{ws}(1'') - p_{wf}(t_p)}{m} + \lg \left(\frac{k}{\phi\mu c_t r_w^2} \right) + 0.35137 \right]. \quad (3.21)$$

Using field units, two constants have to be changed in Equation 3.19 and Equation 3.20:

$$p_{ws} - p_{wf} = -162.6 \frac{q\mu B}{hk} \left[\lg \Delta t + \lg \left(\frac{k}{\phi\mu c_t r_w^2} \right) + 3.2275 + 0.86859s \right]. \quad (3.22)$$

If one substitutes $\Delta t = 1 \text{ hour}$, it follows from Equation 3.22 that

$$s = -1.1513 \left[\frac{p_{ws}(1 \text{ hour}) - p_{wf}(t_p)}{m} + \lg \left(\frac{k}{\phi \mu c_t r_w^2} \right) - 3.2275 \right]. \quad (3.23)$$

Production is rarely constant before shut in. The time t_p is therefore calculated from the cumulative production N_p and from the last production rate:

$$t_p = \frac{N_p}{q}. \quad (3.24)$$

3.4. Reservoir Pressure

In an infinite acting reservoir $Y(t_{Dp})$ is 0, therefore the straight line extrapolated to $(t_p + \Delta t)/\Delta t = 1$, according to Equation 3.6, gives the initial reservoir pressure p_i . For a bounded reservoir, this value is equal to

$$p^* = p_i + \frac{m}{2.3026} Y(t_{Dp}, r_{De}). \quad (3.25)$$

p^* is smaller than p_i , (m is negative!), but larger than the average reservoir pressure \bar{p} , as is shown in Figure 3.2.

If the shut in time is long enough, a complete pressure equalization takes place in the reservoir:

$$\lim_{\Delta t \rightarrow \infty} p_{ws} = \bar{p}. \quad (3.26)$$

It would be very important to know the mean reservoir pressure. Usually, the shut in time is too short to draw the last part of the curve. But the mean pressure can also be determined on the basis of the value p^* by means of the MATTHEWS-BRONS-HAZENBROEK^[10] method, (MBH-plot).

The authors have compiled a series of diagrams, illustrated in Figure 3.3 - Figure 3.4 from which for different shapes of drainage areas the dimensionless pressure value

$$p_{DMBH}(t_{pDA}) = \frac{2.3026(\bar{p} - p^*)}{m} \quad (3.27)$$

can be determined as a function of

$$t_{pDA} = \frac{kt_p}{\phi \mu c_t A}. \quad (3.28)$$

In field units:

$$t_{pDA} = 0.60536 \frac{kt_p}{\phi\mu c_r A}. \quad (3.29)$$

If p^* is known, \bar{p} can be estimated.

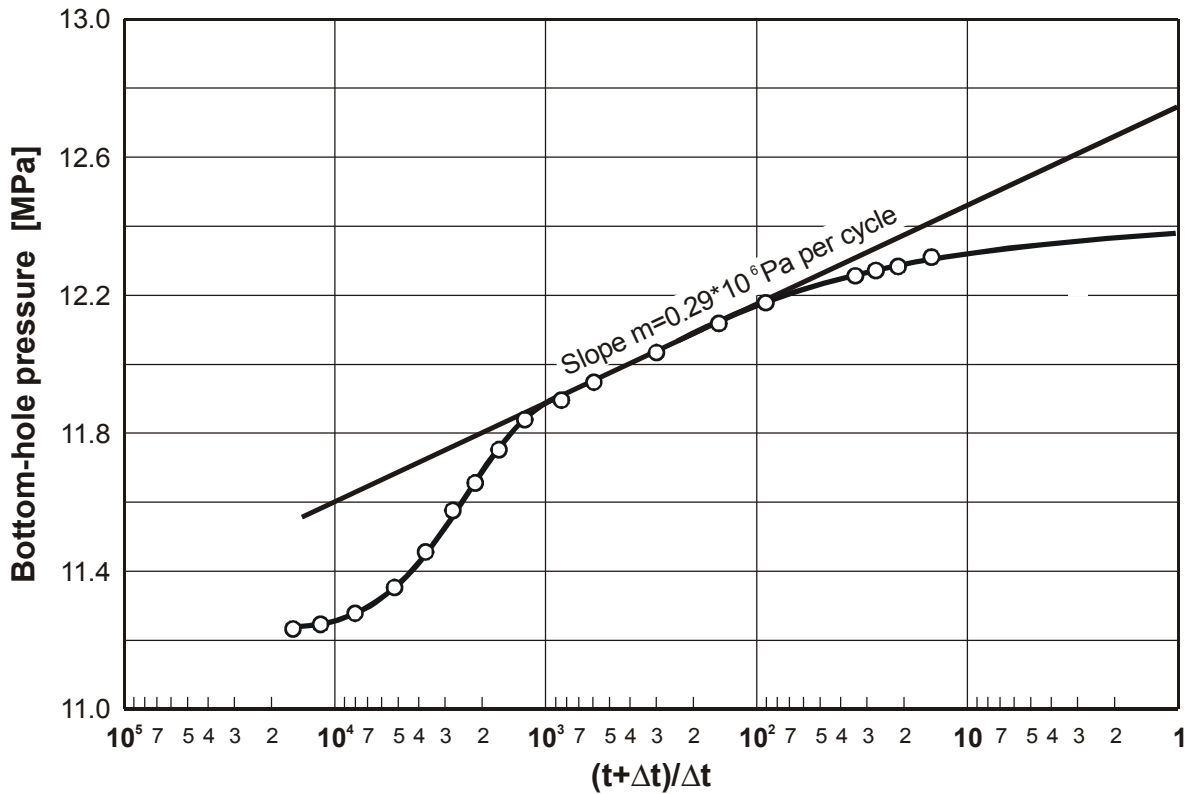


Figure 3.2: Pressure buildup curve with a limited drainage area

Example 3.1

The permeability of the reservoir and the skin factor should be determined on the basis of Figure 3.1 which shows a pressure buildup curve.

Data:

$$\begin{aligned} N_p &= 21409 \text{ m}^3 [134648 \text{ bbl}], \text{ cumulative production} \\ q &= 38.3 \text{ m}^3/\text{d} [241 \text{ bbl}/\text{d}], \text{ production rate before shut in} \\ B_{oi} &= 1.28 [] \\ p_i &= 20.7 \text{ MPa} [3002.3 \text{ psi}] \\ \mu_o &= 9.2 \times 10^{-3} \text{ Pas} [9.2 \text{ cp}] \end{aligned}$$

$$\begin{aligned}
 h &= 21 \text{ m [68.9 ft]} \\
 \phi &= 0.17 [] \\
 S_{wi} &= 0.26 [] \\
 c_t &= 1.2 \times 10^{-9} \text{ Pa}^{-1} [8.27 \times 10^{-6} \text{ 1/psi}] \\
 r_w &= 0.1 \text{ m [0.328 ft]}
 \end{aligned}$$

Solution:

The production time according to Equation 3.24, is

$$t_p = \frac{N_p}{q} = \frac{21409}{38.3} = 559 \text{ days} \cong 13400 \text{ hours} \cong 4.824 \times 10^7 \text{ s}.$$

The slope of the straight line in Figure 3.1 is

$$m = \frac{\Delta p}{\text{Cycle}} = (14.378 - 14.456) \times 10^6 = -78 \times 10^3 \text{ Pa [-11.31 psi]}.$$

From Equation 2.15:

$$k = 0.183 \frac{q \mu B}{hm} = 0.183 \frac{-38.3 \times 1.28 \times 9.2 \times 10^{-3}}{86400 \times 21(-78 \times 10^3)} = 0.583 \times 10^{-12} \text{ m}^2.$$

The skin effect from Equation 3.21 is for

$$p_{ws}(1 \text{ hour}) = 14.272 \text{ MPa},$$

$$p_{wf} = 13.534 \text{ MPa},$$

$$\begin{aligned}
 s &= -1.1513 \left[\frac{(14.272 - 13.534) \times 10^6}{-0.078 \times 10^6} + \lg 3600 + \right. \\
 &\quad \left. + \lg \left(\frac{0.583 \times 10^{-12}}{0.17 \times 9.2 \times 10^{-3} \times 1.2 \times 10^{-9} \times 0.1^2} \right) + 0.35137 \right] \\
 &= -1.1513[-9.4615 + 3.5563 + 1.4924 + 0.35137] = 4.7.
 \end{aligned}$$

In field units:

$$k = 162.6 \frac{q\mu B}{hm} = 162.6 \frac{-241 \times 1.28 \times 9.2}{68.9 \times (-11.31)} = 593.3 \text{ md}.$$

The skin effect from Equation 3.23 is for

$$p_{ws}(1 \text{ hour}) = 2070 \text{ psi},$$

$$p_{wf} = 1962 \text{ psi},$$

$$s = -1.1513 \left[\frac{(2070 - 1962)}{-11.31} + \lg \left(\frac{592.2}{0.17 \times 9.2 \times 1172 \times 10^{-4} \times 0.3281^2} \right) - 3.2255 \right]$$

$$= -1.1513 [-9.54 + 8.6297 - 3.2275] = 4.77 .$$

Example 3.2

The straight line of the pressure buildup curve from Figure 3.1 extrapolated to $t_p + \Delta t / (\Delta t) = 1$, yields $p^* = 14.594 \text{ MPa}$ [2116.1 psi].

Data:

$$N_p = 21409 \text{ m}^3 \text{ [134648 bbl]}, \text{ cumulative production}$$

$$q = 38.3 \text{ m}^3/\text{d} \text{ [241 bbl/d]}, \text{ production rate before shut in}$$

$$B_{oi} = 1.28 \text{ []}$$

$$p_i = 20.7 \text{ MPa} \text{ [3002.3 psi]}$$

$$\mu_o = 9.2 \times 10^{-3} \text{ Pas} \text{ [9.2 cp]}$$

$$h = 21 \text{ m} \text{ [68.9 ft]}$$

$$\phi = 0.17 \text{ []}$$

$$S_{wi} = 0.26 \text{ []}$$

$$c_t = 1.7 \times 10^{-8} \text{ Pa}^{-1} \text{ [1.172} \times 10^{-4} \text{ 1/psi]}$$

$$r_w = 0.1 \text{ m} \text{ [0.328 ft]}$$

The drainage area is a square with a surface $A = 0.42 \times 10^6 \text{ m}^2$ [103.8 acre]. The well is placed in the center. The mean pressure of the drainage area is to be determined.

Solution:

According to Equation 1.3,

$$t_{pDA} = \frac{kt_p}{\phi\mu c_t A} = \frac{0.583 \times 10^{-12} \times 4.824 \times 10^7}{0.17 \times 9.2 \times 10^{-3} \times 1.7 \times 10^{-8} \times 0.42 \times 10^6} = 2.518$$

and for this value from Figure 3.4

$$p_{DMBH} = 2.3026(p^* - \bar{p})/m = 4.35.$$

From Figure 3.1

$$m = \frac{\Delta p}{\text{Cycle}} = -0.078 \text{ MPa},$$

and therefore

$$\bar{p} = p^* + \frac{m \times p_{DMBH}}{2.3026} = 14.594 \times 10^6 + \frac{(-0.078 \times 10^6) \times 4.35}{2.3026} = 12.3 \times 10^6 \text{ Pa}.$$

In field units:

$$t_{pDA} = \frac{0.60536 \times 10^{-8} kt}{\phi\mu c_t A} = \frac{0.60536 \times 10^{-8} \times 592.2 \times 13400}{0.17 \times 9.2 \times 1.172 \times 10^{-4} \times 103.8} = 2.52,$$

$$m = \frac{\Delta p}{\text{Cycle}} = -11.31 \text{ psi}.$$

Therefore,

$$\bar{p} = p^* + \frac{m \times p_{DMBH}}{2.3026} = 2116.1 + \frac{(-11.31) \times 4.35}{2.3036} = 2094.7 \text{ psi}.$$

3.5. Gas Producing Wells

Below the bubble point, the gas is dissolved in the reservoir. The evaluation of the pressure buildup curve is carried out as before. However, the total two-phase compressibility and the total mobility are applied.

From the slope of the pressure buildup curve one can also determine hk_g :

$$hk_g = 0.183 \frac{q_{gf} \mu_{gf} B_g}{m}, \tag{3.30}$$

where

$$q_{gf} = q_g - q_o R_s.$$

After shut in however, the pressure increases in the vicinity of the well, whereas the gas saturation decreases. This fact is expressed by an *apparent skin*. If this effect is disregarded, one could easily fail and order unnecessary formation treatments.

For gas wells, an apparent skin factor s' is determined and includes the influence of the turbulent flow. According to Equation 1.65,

$$s' = s + D|q|. \tag{3.31}$$

In both cases, the actual skin factor can be determined from two pressure buildup curves with different production rates. s' is drawn as a function of q , and the value extrapolated to $q = 0$ gives the correct skin factor.

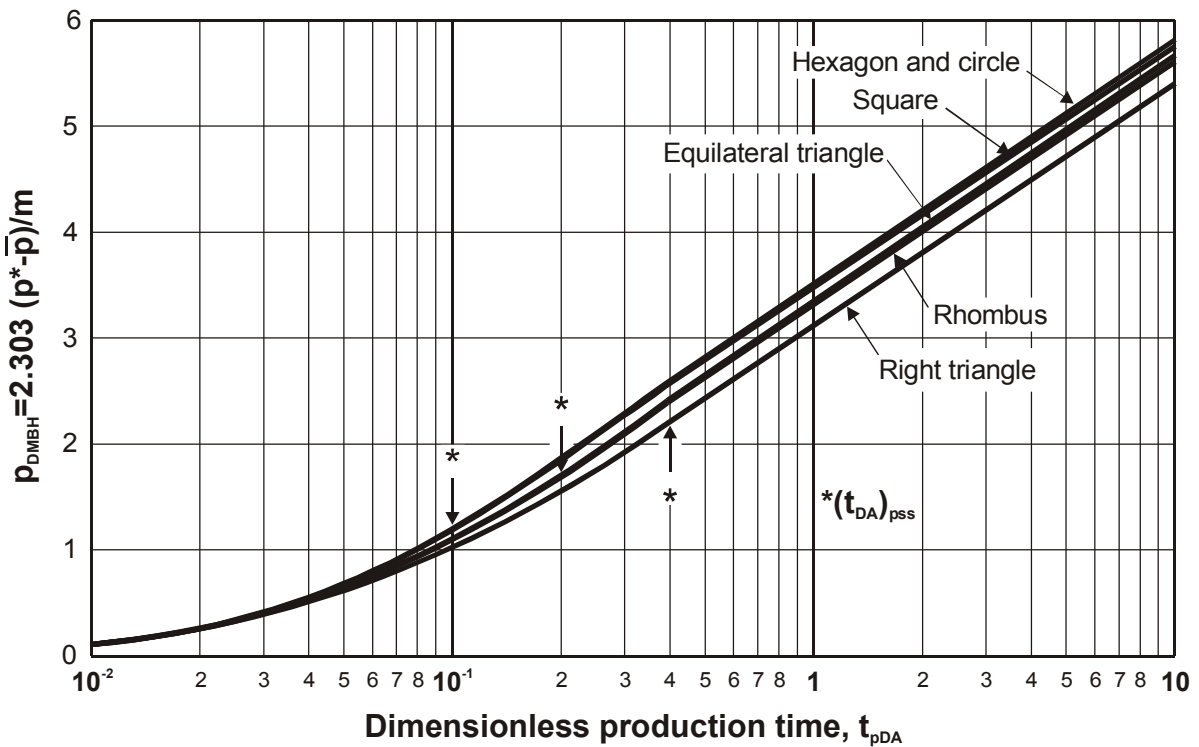


Figure 3.3: MBH dimensionless pressure for a well in the center of equilateral drainage areas (after MATTHEWS-BRONS-HAZENBROEK^[10])

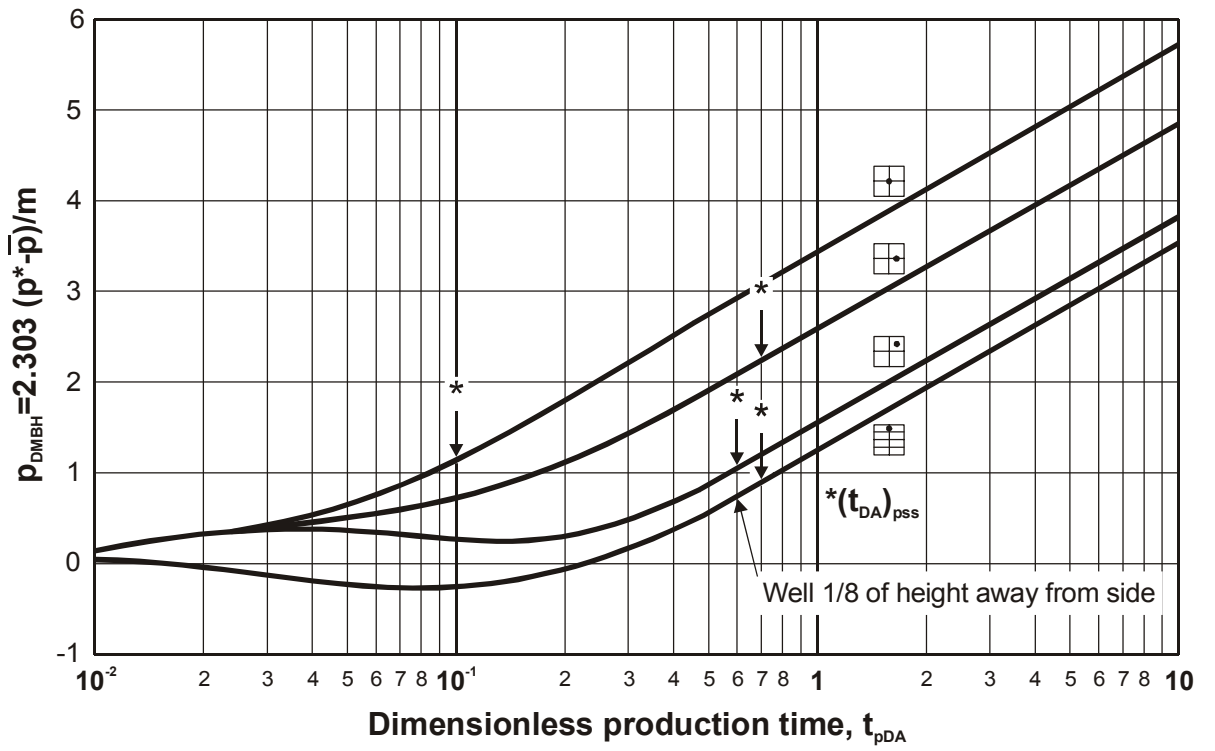


Figure 3.4: MBH dimensionless pressure for different well locations in a square drainage area (after MATTHEWS-BRONS-HAZENBROEK^[10])

4 Multiple Well Testing

Two or more wells are required for the test. One well is active, the others serve as observation wells. In the active well, production (or injection) takes place in the given way. The observation wells are closed. The pressure changes in these wells are recorded.

There exists a variety of multiple well testing methods, two of them are discussed here:

- interference test (long time interference testing),
- pulse test.

With an interference test, the rate of the active well is modified. For example, the well is closed or put into operation and the effects on the observation wells are measured (Figure 1.6). From this, information about the formation properties between the wells is derived. The same purpose is achieved with pulse tests, but within a considerably shorter time (Figure 1.7). The pressure changes are small, sometimes only to an extent of kPa , therefore special differential pressure gauges are needed.

4.1. Interference Test

The distance between the active well and the observation wells is r . The simplest, of course, is to have the active well closed for an extended period of time and then put it into operation (at time $t = 0$). Equation 1.37 gives the dimensionless pressure function. For this case, it is presented graphically in Fig. 1.8. For a more complicated production history, the superposition principle must be used for constructing a type curve.

The measurement is evaluated with the type curve matching method, similarly as in section 3.2. In this case, the type curve is identical to Fig. 1.8. Fig. 4.1 illustrates the procedure.

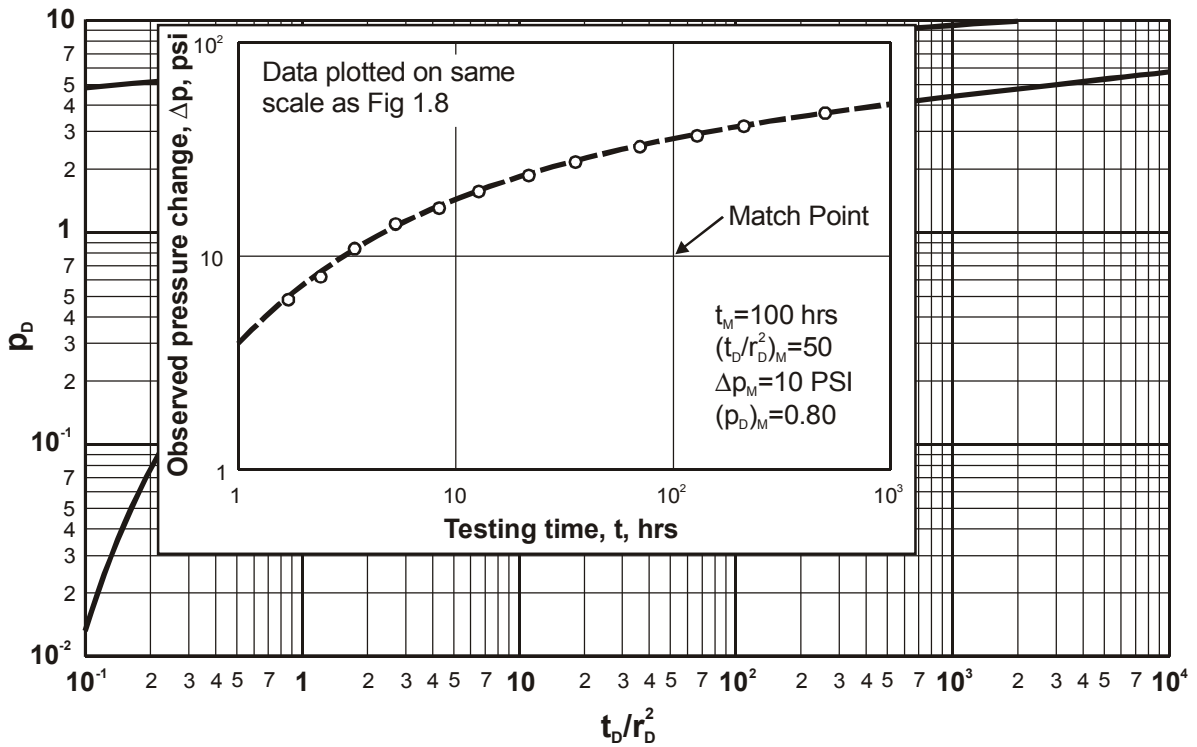


Figure 4.1: Illustration of type curve matching for an interference test (after EARLOUGHER^[4])

From the *match point*:

$$k = \frac{q\mu B(p_D)_M}{2\pi h \Delta p_M}, \tag{4.1}$$

$$\phi c_t = \frac{k}{\mu r^2} \frac{t_M}{(t_D/r_D^2)_M}. \tag{4.2}$$

In field units:

$$k = 141.2 \frac{q\mu B(p_D)_M}{h \Delta p_M}, \tag{4.3}$$

$$\phi c_t = \frac{0.0002637k}{\mu r^2} \frac{t_M}{(t_D/r_D^2)_M}. \tag{4.4}$$

If the active well is shut in at time t_1 , a pressure buildup follows in the observation well. The difference between the extrapolated pressure curve from the production period and the measured values is now drawn as a function of $t - t_1$ and evaluated as above. The same procedure is followed if the interference is caused by the shut in of an active well.

Example 4.1

During an interference test, water was injected in the active well for 22 days. The distance to the observation well is 112.4 m [368.8 ft]. The measured pressure changes are given in the following table:

Time t	Δp	
	kPa	psi
1.70	560	8120
2.35	710	10295
3.40	930	13485
5.40	1150	16675
8.40	1400	20300
13.00	1650	23925
22.00	1920	27840
36.00	2300	33350
72.00	2750	39875
132.00	3050	44225
216.00	3400	49300
528.00	3900	56550

$$q = 300 \text{ m}^3/d [1887 \text{ bbl}/d]$$

$$\mu = 0.82 \times 10^{-3} \text{ Pas} [0.82 \text{ cp}]$$

$$B_w = 1.0$$

$$h = 12 \text{ m} [39.4 \text{ ft}]$$

$$r = 112.4 \text{ m} [368.8 \text{ ft}]$$

The permeability and the product ϕc_t of the reservoir are to be determined.

Solution:

The measured p-values are drawn on a transparent sheet vs. t (hour), and matched by parallel shifting in Figure 4.1 with the type curve in Figure 1.8. In the match point:

$$t_M = 100 \text{ hours}, \quad (t_D/r_D^2)_M = 50,$$

$$\Delta p_M = 10^5 \text{ Pa} [14.5 \text{ psi}], \quad (p_D)_M = 0.80.$$

From Equation 4.1 and Equation 4.2,

$$k = \frac{q\mu B (p_D)_M}{2\pi h \Delta p_M} = \frac{300 \times 1.0 \times 0.82 \times 10^{-3} \times 0.8}{86400 \times 2\pi \times 12 \times 10^5} = 0.302 \times 10^{-12} \text{ m}^2,$$

$$\phi c_t = \frac{k}{\mu r^2} \frac{t_M}{(t_D/r_D^2)_M} = \frac{0.302 \times 10^{-12}}{0.82 \times 10^{-3} \times 112.4^2} \frac{100 \times 3600}{50} = 0.21 \times 10^{-9} \text{ Pa}^{-1}.$$

In field units:

$$k = 141.2 \frac{1887 \times 1.0 \times 0.82}{39.4} \frac{0.8}{14.5} = 306 \text{ mD},$$

$$\phi c_t = \frac{0.0002637 \times 306 \times 100}{0.82 \times 368.8^2 \times 50} = 0.15 \times 10^{-6} \text{ psi}^{-1}.$$

4.2. Pulse Test

In this process the active well produces at short intervals (Figure 4.2). The production and shut in periods are different, but the cycles must be the same. The ratio of pulse time Δt_p and cycle time Δt_c is

$$F' = \frac{\Delta t_p}{\Delta t_c}. \quad (4.5)$$

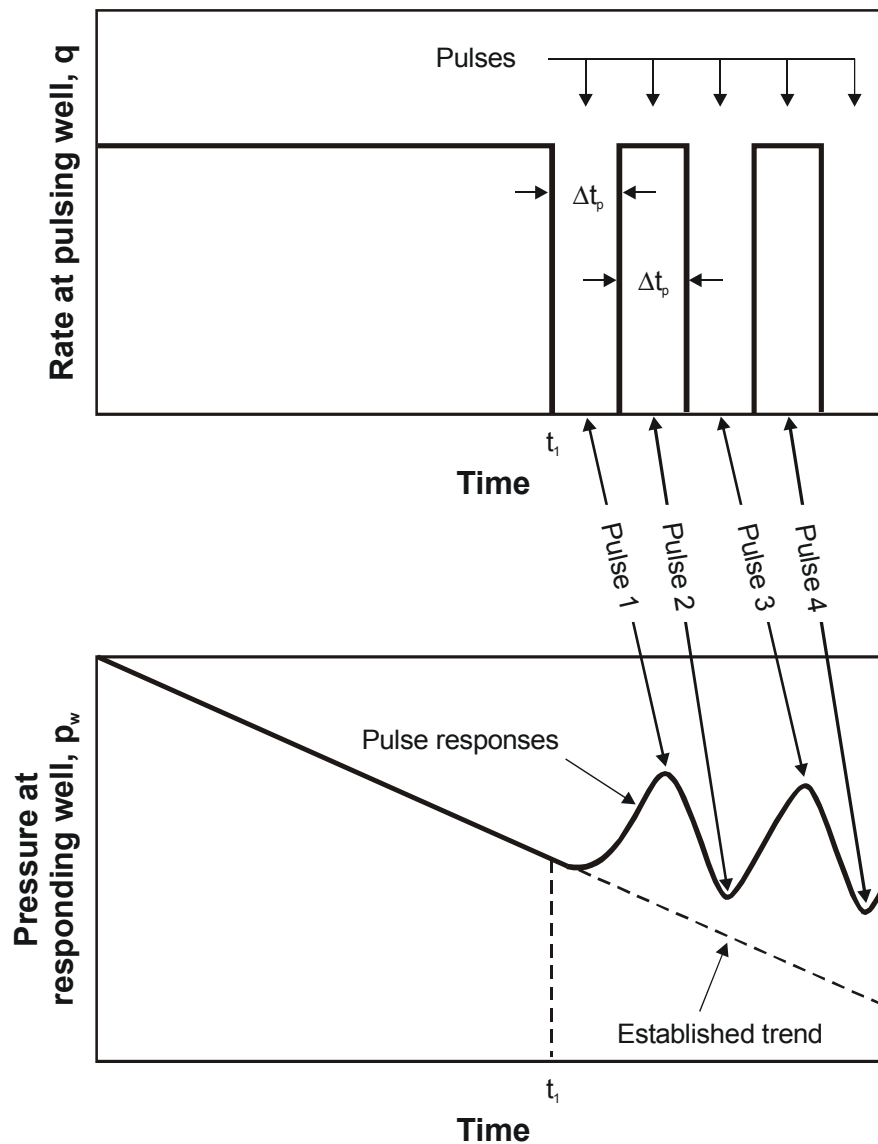


Figure 4.2: Schematic illustration of rate (pulse) history and pressure response for a pulse test

The pressure change in the observation well is the result of a general trend and the pulsation. A tangent is drawn to the maximum and the minimum of the pressure waves, as shown in Figure 4.3, and the time lags t_{L1} , t_{L2} , t_{L3} and the pressure differences Δp_1 , Δp_2 , Δp_3 are measured.

If the cycle time Δt_c is short, the evaluation will be very unreliable. If it is long, however, unnecessary costs are incurred. Therefore, the pulse test must be carefully planned.

Since the pulse times are short, the formation can be considered as infinite. The dimensionless pressure function is calculated by the superposition of the elementary solution according to Equation 1.37.

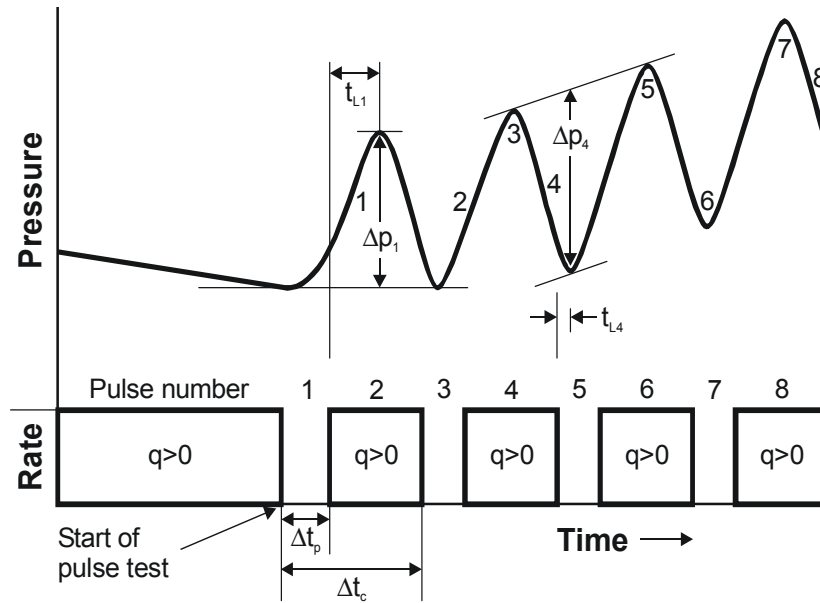


Figure 4.3: Schematic pulse-test rate and pressure history showing definition of time and pulse response amplitude.

KAMAL and BRIGHAM^[7] have carried out this task, the results are comprised in the diagrams Figure 4.4 to Figure 4.11. There are special diagrams for the first and second pulses and for all following odd pulses (3., 5., ...) and even pulses (4., 6., ...).

The evaluation is very simple. On the basis of $t_L/\Delta t_c$ and F' , the value $\Delta p_D t_L/\Delta t_c^2$ can be read from Figure 4.4 to Figure 4.7 and from Equation 4.1

$$k = \frac{q\mu B(\Delta p_D [t_L/\Delta t_c]^2)_{Fig}}{2\pi h \Delta p [t_L/\Delta t_c]^2} \tag{4.6}$$

From Figure 4.8 to Figure 4.11, $[(t_L)_D/r_D^2]_{Fig}$ can be read, and from Equation 4.2 to Equation 4.4 follows:

$$\phi c_t = \frac{kt_L}{\mu r^2 [(t_L)_D/r_D^2]_{Fig}} \tag{4.7}$$

$$k = 141.2 \frac{q\mu B(\Delta p_D [t_L/\Delta t_c]^2)_{Fig}}{h \Delta p [t_L/\Delta t_c]^2} \tag{4.8}$$

$$\phi c_t = \frac{0.0002637kt_L}{\mu r^2 [(t_L)_D/r_D^2]_{Fig}} \tag{4.9}$$

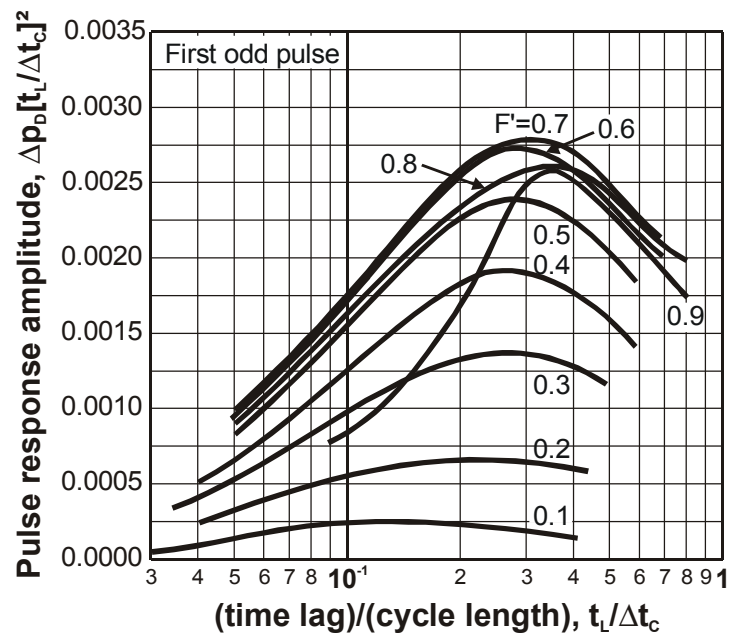


Figure 4.4: Pulse testing: relation between time lag and response amplitude for first odd pulse (after KAMAL and BRIGHAM^[7])

The evaluation is performed for all cycles and the mean value of the results is calculated.

Example 4.2

A pulse test is to be carried out in an undersaturated oil reservoir. Distances of wells are $r = 175$ m [574 ft].

The reservoir data:

$$h = 20 \text{ m [65.6 ft]}$$

$$B_o = 1.10$$

$$\mu_o = 2 \times 10^{-3} \text{ Pas [2 cp]}$$

$$r_w = 0.1 \text{ m [0.328 ft]}$$

The following values are estimated:

$$c_t = 10^{-9} \text{ Pa}^{-1} [0.6896 \times 10^{-5} \text{ 1/psi}]$$

$$\phi = 0.2$$

$$k = 0.1 \times 10^{-12} \text{ m}^2 [100 \text{ mD}]$$

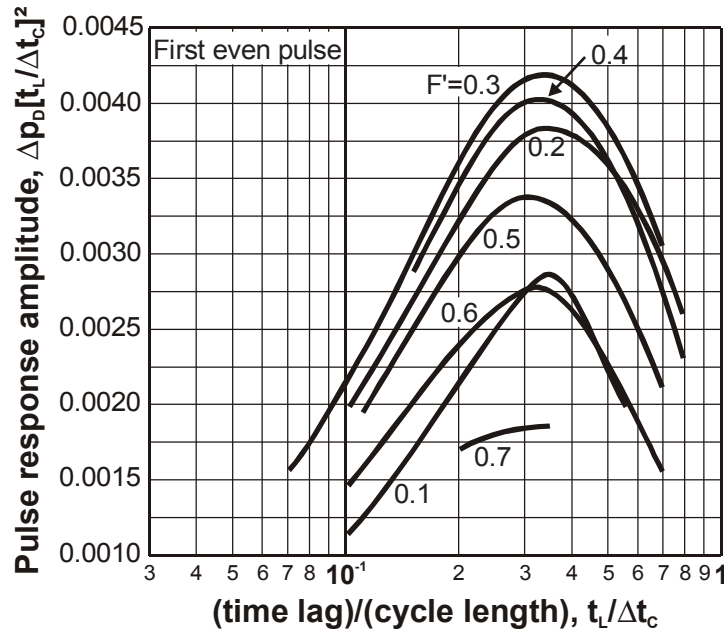


Figure 4.5: Pulse testing: relation between time lag and response amplitude for first even pulse (after KAMAL and BRIGHAM^[7])

Solution:

a.) Planning of the test: the cycle time and the production rate are to be determined. Based on experience, it is favorable if the time lag is 1/3 of the cycle time:

$$t_L / t_c = 1/3 .$$

We select

$$F' = \frac{\Delta t_p}{\Delta t_c} = 0.5 ,$$

and from Fig. 4.8

$$[(t_L)_D / r_D^2]_{Fig} = 0.09 .$$

From Eq. 4.7

$$\begin{aligned} \Delta t_c &= 3t_L = 3 \frac{\phi c_t \mu r^2 [(t_L)_D / r_D^2]_{Fig}}{k} \\ &= \frac{3 \times 0.2 \times 10^{-9} \times 2 \times 10^{-3} \times 175^2 \times 0.09}{0.1 \times 10^{-12}} \approx 33075 \text{ s} \approx 9 \text{ hours} \end{aligned}$$

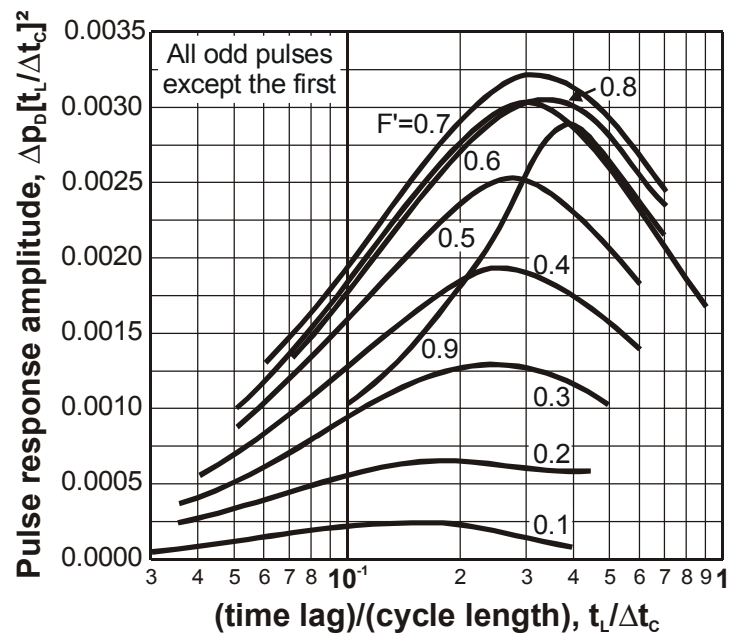


Figure 4.6: Pulse testing: relation between time lag and response amplitude for all odd pulses except the first pulse (after KAMAL and BRIGHAM^[7])

In field units:

$$\Delta t_c = 3t_L = \frac{3 \times 0.2 \times 0.6896 \times 10^{-5} \times 2 \times 574^2 \times 0.09}{0.0002637 \times 100} = 9.3 \text{ hours}.$$

The accuracy of the used differential pressure gauge is 20 Pa [0.003 psi], therefore the pressure differences have to be at least 2000 Pa [0.3 psi] in order to be sure that the error is less than 1%. From Figure 4.4

$$\Delta p_D [t_L / \Delta t_c]^2 = 0.00238$$

and from Equation 4.6

$$\begin{aligned} q &= \frac{2\pi h k \Delta p [t_L / \Delta t_c]^2}{\mu B (\Delta p_D [t_L / \Delta t_c]^2)_{Fig}} = \\ &= \frac{2\pi \times 20 \times 0.1 \times 10^{-12} \times 2000 \times (1/3)^2}{1.1 \times 2 \times 10^{-3} \times 0.00238} = 5.33 \times 10^{-4} \text{ m}^3 \text{ s}^{-1} = 46 \text{ m}^3 / \text{d}. \end{aligned}$$

In field units:

$$q = \frac{hk\Delta p [t_L / \Delta t_c]^2}{141.2 \times \mu B (\Delta p_D [t_L / \Delta t_c]^2)_{Fig}} = \frac{65.6 \times 100 \times 0.3 \times (1/3)^2}{141.2 \times 1.1 \times 2 \times 0.00238} = 295.8 \text{ bbl/d.}$$

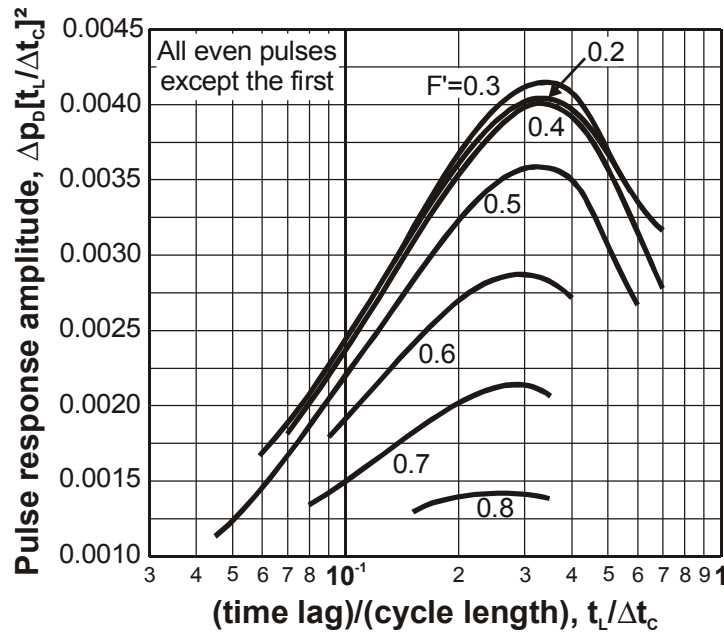


Figure 4.7: Pulse testing: relation between time lag and response amplitude for all even pulses except the first pulse (after KAMAL and BRIGHAM^[7])

b.) The test was performed in the following way:

- Cycle time: 8 hours
- Rate: 48 m³/d [302 bbl/d]
- First pressure change Δp1: 1700 Pa [0.246 psi]
- First time log t_{L1}: 12860 s = 3.572 hours

$$\frac{t_{L1}}{\Delta t_c} = \frac{12860}{8 \times 3600} = 0.446.$$

From Figure 4.4 and Figure 4.8,

$$\Delta p [t_L / \Delta t_c]^2 = 0.002175,$$

$$(t_L)_D / r_D^2 = 0.086,$$

and from Equation 4.6 and Equation 4.7,

$$k = \frac{48 \times 1.1 \times 2 \times 10^{-3} \times 0.002175}{86400 \times 2\pi \times 20 \times 1700 \times 0.446^2} = 0.062 \times 10^{-12} \text{ m}^2,$$

$$\phi c_t = \frac{0.062 \times 10^{-12} \times 12860}{2 \times 10^{-3} \times 175^2 \times 0.086} = 0.153 \times 10^{-9} \text{ Pa}^{-1}.$$

In field units:

$$k = 141.2 \frac{302 \times 1.1 \times 2 \times 0.002175}{65.6 \times 0.246 \times 0.446^2} = 63.6 \text{ mD},$$

$$\phi c_t = \frac{0.0002637 \times 63.6 \times 3.572}{2 \times 574^2 \times 0.086} = 0.105 \times 10^{-5} \text{ psi}^{-1}.$$

The following pulses are evaluated in the same way. The mean values of k and ϕc_t can be used as the best estimates.

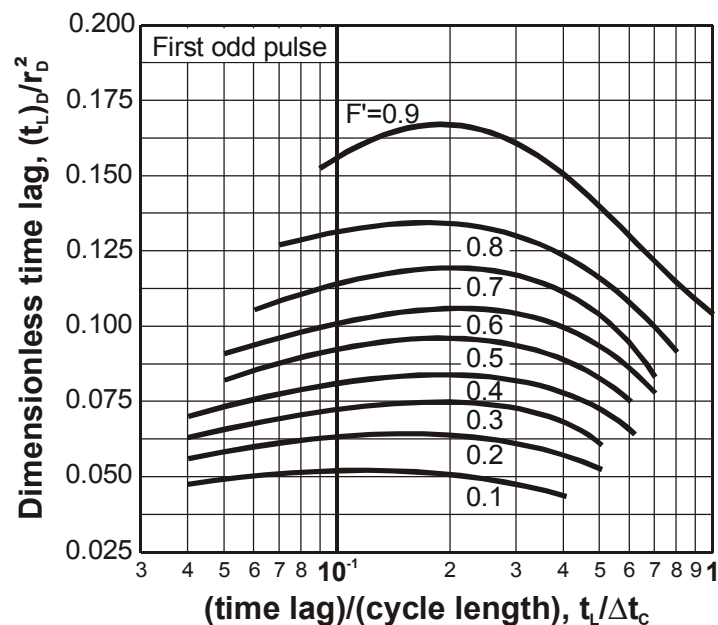


Figure 4.8: Pulse testing: relation between time lag and cycle length for the first odd pulse (after KAMAL and BRIGHAM^[7])

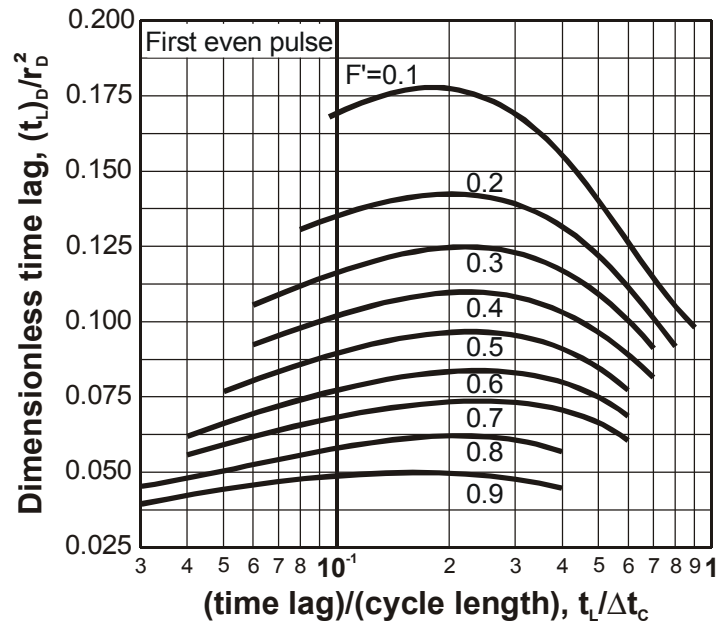


Figure 4.9: Pulse testing: relation between time lag and cycle length for the first even pulse (after KAMAL and BRIGHAM^[7])

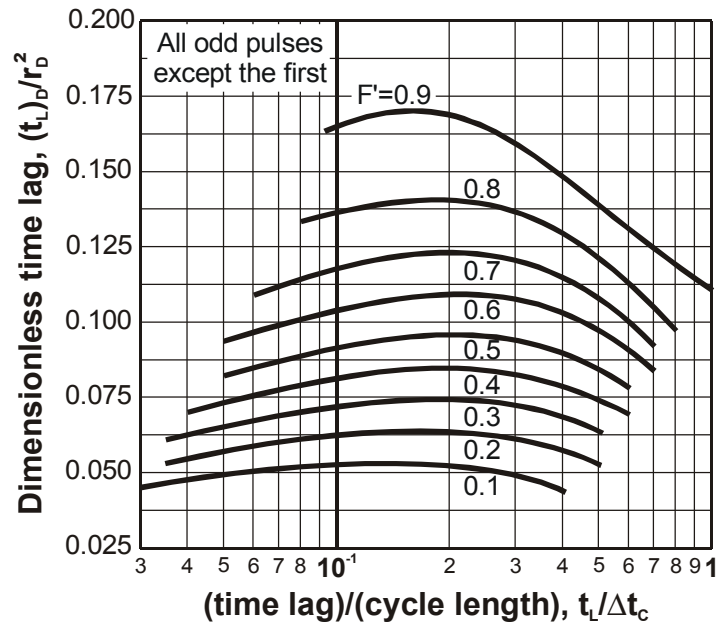


Figure 4.10: Pulse testing: relation between time lag and cycle length for all odd pulses except the first pulse (after KAMAL and BRIGHAM^[7])

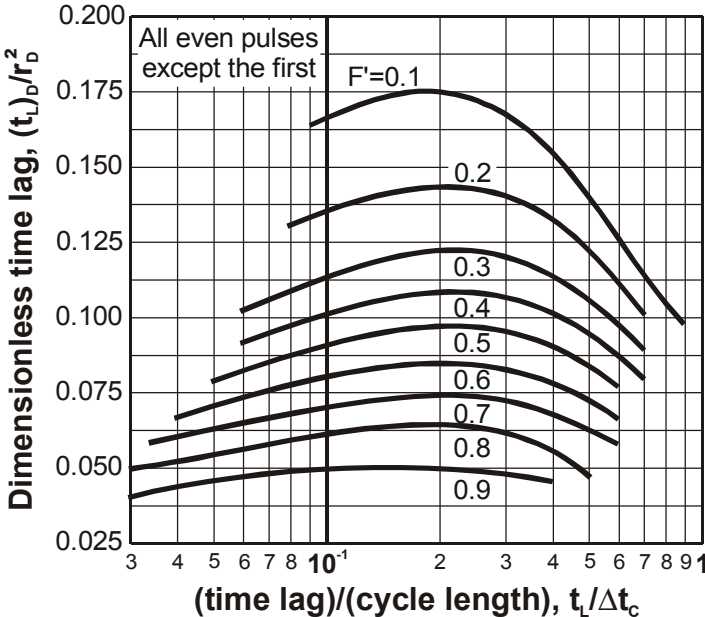


Figure 4.11: Pulse testing: relation between time lag and cycle length for all even pulses except the first pulse (after KAMAL and BRIGHAM^[7])

5 Nomenclature

A	area	L^2
B	formation volume factor	
B_g	formation volume factor, gas	
B_o	formation volume factor, oil	
C	wellbore storage constant	L^4t/m
C_A	shape factor (Eq. 1.46)	
C_D	dimensionless wellbore storage constant	
c	compressibility	Lt^2/m
c_t	total compressibility	Lt^2/m
D	turbulence factor	t/L^3
DF	damage factor	
$-Ei(-z)$	exponential integral, x positive	
FE	flow efficiency	
G	fluid mass	m
g	acceleration of gravity	L/t^2
h	bed thickness, individual	L
J	productivity index	L^4t/m
k	permeability, absolute (fluid flow)	L^2
k_g	effective permeability to gas	L^2
k_o	effective permeability to oil	L^2
k_{rg}	relative permeability to gas	
k_{ro}	relative permeability to oil	
k_{rw}	relative permeability to water	
k_w	effective permeability to water	L^2
L	distance, length, or length of path	L
m	slope	m/Lt^2 or m/Lt^3
$m(p)$	real gas pseudo pressure	
N_p	cumulative oil production	L^3
p_i	pressure, initial	m/Lt^2
p_{wf}	pressure, bottomhole flowing	m/Lt^2
p_{ws}	pressure, bottomhole, at any time after shut-in	m/Lt^2
q	production rate or flow rate	L^3/t
q_D	production rate, dimensionless	
q_o	production rate, oil	L^3/t
q_w	production rate, water	L^3/t
R_s	solution gas / oil ratio	
r	radius	L
r_e	outer radius	L
r_w	well radius	L
S_{wi}	initial water saturation	
s	skin effect	
t	time	t
Δt	shut in time	t
Δ_c	cycle time	t

t_D	dimensionless time (Eq. 1.2)	
t_D	time, dimensionless	
t_{DA}	dimensionless time (Eq. 1.3)	
t_p	time well was on production prior to shut-in, equivalent (pseudotime)	t
t_L	log time	t
V	volume	L^3
Z	gas compressibility factor	L^3

Greek letters

μ	viscosity, dynamic	m/Lt
μ_g	viscosity, gas	m/Lt
μ_o	viscosity, oil	m/Lt
μ_w	viscosity, water	m/Lt
ρ	density	m/L^3
ϕ	porosity	

Subscripts

D	dimensionless
g	gas
gf	free gas
i	initial
o	oil phase
r	relative
s	skin
sc	standard condition
sf	sand face
w	water
w	well
wf	well under flowing condition
ws	well under shut-in conditions

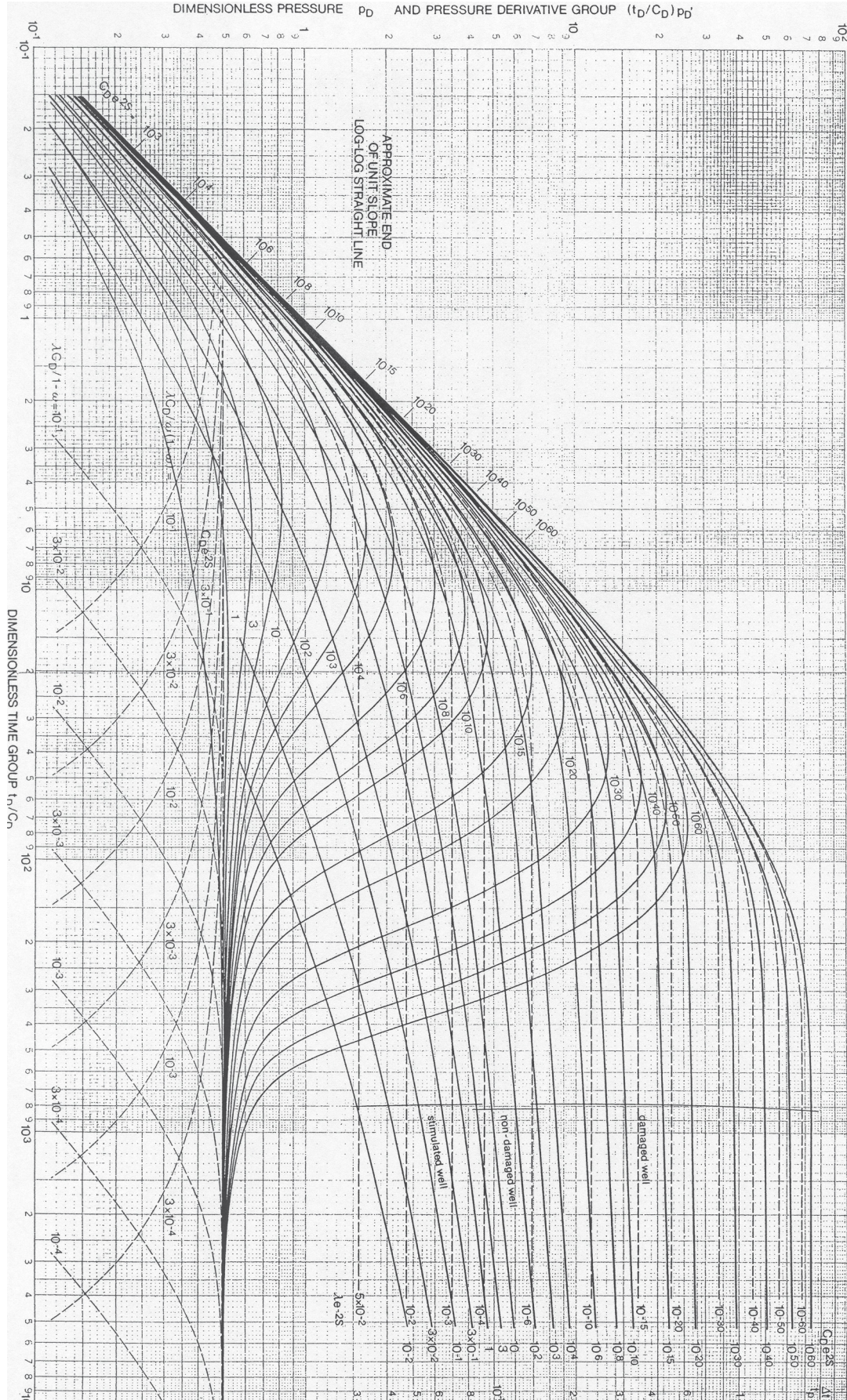
6 References

- 1 Al-Hussainy, R., Ramey, H.J. JR. and Crawford, P.B. (1966): "The Flow of Real Gases Through Porous Media," J.Pet.Tech. (May 1966) 624-626, Trans., AIME (1966) 237.
- 2 Bourdet, D. et al. (1983): "A New Set of Type Curves Simplifies Well Test Analysis," World Oil (May 1983), 95-106.
- 3 Bourdet, D. et al. (1984): "New Type Curves Aid Analysis of Fissured Zone Well Tests," World Oil (April 1984).
- 4 Earlougher, R. C., Jr. (1977): "Advances in Well Test Analysis," Monographs Series, Soc. Pet. Eng. (1977), Trans., AIME, 5, Dallas.
- 5 Earlougher, R.C., Jr., and Ramey, H.J., Jr. (1973): "Interference Analysis in Bounded Systems," J. Cdn. Pet. Tech. (Oct.-Dec. 1973) 33-45.
- 6 Heinemann, Z.E.: "Fluid Flow in Porous Media" Texbook, Montanuniversität Leoben, (2003) p.190.
- 7 Kamal, M. and Brigham, W.E. (1975): "Pulse-Testing Response for Unequal Pulse and Shut-In Periods," Soc. Pet. Eng. J. (Oct. 1975) 399-410, Trans., AIME, 259.
- 8 Lee, John: "Well Testing," SPE Texbook Series, Vol.1. Dallas (1982), p. 159.
- 9 Martin, J.C. (1959): "Simplified Equations of Flow in Gas Drive Reservoirs and the Theoretical Foundation of Multiphase Pressure Buildup Analyses," Trans., AIME (1959) 216, 309-311.
- 10 Matthews, C.S., Brons; F., and Hazenbrock, P. (1954): "A Method for Determination of Average Pressure in a Bounded Reservoir, "Trans., AIME (1954) 201, 182-189.
- 11 Matthews, C.S. and Russel, D.G. (1967): "Pressure Buildup and Flow Tests in Wells," Monograph Series, Soc. of Pet. Eng. of AIME, 1, Dallas.
- 12 Miller, C.C., Dyes, A.B., and Hutchinson, C.A., Jr. (1950): "The Estimation of Permeability and Reservoir Pressure From Bottom Hole Pressure Build-Up Characteristics," Trans., AIME (1950) 189, 91-104.
- 13 Perrine, R.L. (1956): "Analysis of Pressure Buidup Curves," Drill. and Prod. Prac., API (1956), 482-509.
- 14 Ramey, H.J., Jr. (1965): "Non Darcy Flow and Wellbore Storage Effects in Pressure Build-up and Drawdown of Gas Wells," J. Pet. Tech. (Feb. 1965) 223-233, Trans., AIME, 234.
- 15 Rammey, H.J., Jr. and Cobb, W., M. (1971): "A General Buildup Theory for a Well in a Closed Drainage Area," J.Pet. Tech. (Dec. 1971), 1493-1505.

7 Appendix

WELL WITH WELLBORE STORAGE AND SKIN INFINITE ACTING RESERVOIR WITH DOUBLE POROSITY BEHAVIOR - pseudo steady state interporosity flow
 The use of this type-curve is described in World Oil - October 1983 : INTERPRETING WELL TESTS IN FRACTURED RESERVOIRS by D. BOURDET, J.A. AYOUB, T.M. WHITTLE, Y.M. PIRARD, V.KNIAZEFF.

$\lambda = \alpha r_w^2 \frac{k_m}{k_f}$ FOR OIL — $p_D = \frac{kh}{141.2B\mu} \Delta p$ FOR GAS — $p_D = \frac{kh}{5.030 \cdot 10^4 q} \frac{T_{sc}}{T} \frac{2}{p} \sqrt{\frac{p_0 + \Delta p}{p}} \frac{\mu(p) Z(p)}{\mu(p) Z(p)}$ $\frac{1}{C_D} = \frac{0.8936 C}{\phi c h r_w^2}$ $\frac{1}{C_D} p_D = \frac{kh}{141.2B\mu} \Delta t \Delta p'$ $\frac{1}{C_D} p_D = \frac{kh}{5.030 \cdot 10^4 q} \frac{T_{sc}}{T} \frac{2}{p} \sqrt{\frac{p_0 + \Delta p}{p}} \frac{\mu(p) Z(p)}{\mu(p) Z(p)}$ $\omega = \frac{(\phi V_{c1})_i}{(\phi V_{c1})_i + (\phi V_{c1})_m}$



M-090134
 © Copyright 1983
 Floerco Johnson,
 All rights reserved.
 Without notice

